Hermite Interpolation with Directed Sets

Robert Baier[1]
Gilbert Perria[2]

December 22, 2008

[1]Chair of Applied Mathematics, University of Bayreuth, D-95440 Bayreuth, Germany, email: robert.baier@uni-bayreuth.de
[2]Via Lepanto 67/c, 09170 Oristano, Italy, email: gilbert.perria@googlemail.com

Abstract

The problem of interpolating a set-valued function with convex images is addressed by means of directed sets. A directed set will be visualised as a usually nonconvex set in $\mathbb{R}^n$ consisitng of three parts, the convex, the concave and the mixed-type part together with its normal directions. In this Banach space, a mapping resembling the Kergin map is established. The interpolating property and error estimates similar to the pointwise case are then shown based on the representation of the interpolant through means of divided differences. A comparison to other set-valued approaches is included. The method developed within the article is extended to the scope of the Hermite interpolation by using the derivative notion in the Banach space of directed sets. Finally, a numerical analysis of the explained technique corroborates the theoretical results.

1 Introduction

Hermite interpolation is still a matter of recent research. To mention some examples (we will give only a few citations), it is applied in the following fields: in the construction of shape preserving interpolation methods with C^1- or C^2-functions (cf. [CM96, Man01]); in bivariate and multivariate interpolation with prescribed values for the function and its directional derivatives (cf. [GS00, GM82, SX95, Sau95, Wal97]); in the interpolation of Bézier curves and patches (cf. [LW04]). Further subjects of research involving Hermite interpolation and divided differences include: terrain modelling and reconstruction as in [HSS03]; the analysis of subdivision schemes incorporating derivative data as in [DL95]; the study of the correlation coefficient of Brownian motion as in [BB04]; the interpolation of α-level sets for fuzzy sets (cf. [GA05, Low90]). Another field of application is the analysis of linear/nonlinear partial differential equations. Here, the Hermite-interpolant, as a function of x for fixed time t, has given function and derivative values of a regular solution $y(\cdot, t)$ of the PDE (cf. [Gru05, BSV68]).

The main difficulties in extending the notation and algorithms to the set-valued case (even in the simplest setting of $\mathcal{C}(\mathbb{R}^n)$, the set of convex compact non-empty subsets of $\mathbb{R}^n$) arise when defining a suitable difference and a suitable derivative. Known approaches like the geometric difference as in [Had50, Pon67, Mar00] or the Demyanov difference as in [RA92, DR95] carry the disadvantage of generating either too small (even empty) or too big (convex) sets. In any case, the space $\mathcal{C}(\mathbb{R}^n)$ will not form a vector space. To overcome these difficulties, embeddings based on the support function respectively equivalence classes of pairs of sets as proposed by Rådström, Hörmander (cf. a discussion and references in [PU02, BF01a]) can be used. The main disadvantage is the lack of a visualisation of differences of embedded convex sets as subsets of $\mathbb{R}^n$. For these reasons, the present work considers another embedding by directed sets introduced in [BF01a, BF01b].

Directed sets are the n-dimensional generalisation of generalised/directed intervals (cf. [Kau80, Mar95]) and provide an embedding of $\mathcal{C}(\mathbb{R}^n)$ into the Banach space $\overrightarrow{\mathcal{D}}^n$ (refer to [BF01a, BF01b]). The embedding admits generalisations of the known set arithmetics like the Minkowski addition and multiplication with non-negative scalars; it also delivers a (possibly non-convex) visualisation for differences of embedded sets from $\mathcal{C}(\mathbb{R}^n)$. Directed sets were successfully applied to calculate and visualise the approximation and derivatives of set-valued maps in [BF01c] and to polynomial Lagrange interpolation in [Per07], exemplified in [BF99].

In this paper, the work [Per07] (Lagrange interpolation with directed sets) is extended to Hermite interpolation. Some of the results achieved in [Pre71, DF90, Pet02, Fil04, Sim08] for polynomial interpolation in Banach spaces can be applied, since $\overrightarrow{\mathcal{D}}^n$ is itself a Banach space. But, the verification of the necessary conditions in [DF90] has not been achieved to this stage and error estimates are not provided in [Pre71] or demand too much regularity as in [Pet02, Fil04, Sim08]. Furthermore, no numerical results of set-valued interpolation are visualised in these works unlike in [Lem95, Per07]. Unlike the proofs in [Per07], we will present simple recursive proofs as well as a representation through means of two components (a lower dimensional directed set together

with a scalar function). In this way, connections to other approaches like piecewise linear set-valued interpolation and interpolation with higher polynomial degree as in [Lem95] are revealed. In this approach, polynomial interpolation with higher degree than one may generate negative weights; the interpolating polynomial of the support function is then no longer convex with respect to the direction and additional geometric assumptions have therefore to be posed to ensure the non-emptiness of the sets. The use of directed sets generates interpolating polynomials for which the visualised values are supersets of the ones generated by the approach of [Lem95] with support functions only. Moreover, recursive proofs will show how the Hermite interpolation of directed sets should be implemented in a computer program.

Section 2 serves as an introduction to the basic notions such as: set arithmetics, metrics for convex compact sets in $\mathbb{R}^n$, in particular the Hausdorff and the Demyanov metric as well as the Banach space $\overrightarrow{\mathcal{D}}^n$ of the directed sets which constitutes the main tool within this work. A directed set is parametrised by unit vectors in $\mathbb{R}^n$ and it associates to each direction l a pair consisting of a $(n-1)$-dimensional directed set $\overrightarrow{A_{n-1}(l)} \in \overrightarrow{\mathcal{D}}^{n-1}$ and a scalar $a_n(l) \in \mathbb{R}$. The embedding J_n in [BF01a] from the cone of the convex compact subsets of $\mathbb{R}^n$ into $\overrightarrow{\mathcal{D}}^n$ is recalled. It preserves well-known arithmetic set operations, in particular the Minkowski-addition and the multiplication of sets with non-negative scalars. Moreover, an inverse with respect to addition in $\overrightarrow{\mathcal{D}}^n$ is well-defined and the visualisation of directed sets is also provided. The section following is intended to acquaint the reader with a notion for differentiability of *convex-valued* set-valued maps, i.e. with the notion of *directed differentiability.* In order to properly define the mentioned notion, the function with embedded images is required to be differentiable in the usual sense (seen as a mapping between Banach spaces).

In Section 4 the notations for the divided differences and polynomial interpolation as well as basic facts are recalled and specialised to the directed sets. Therein, the fact that the divided differences and the interpolation act separately on the two components of the function values (directed sets) is highlighted. The *Hermite-Genocchi* formula and an estimate for divided differences and the remainder term of the interpolating polynomial are presented. Following on, the interpolating map $\mathcal{K}_\Theta F$ is introduced in Section 5 and some remainder formulae are illustrated which generalise well-known error estimates to the set-valued case. Piecewise Hermite interpolation of sets and error estimates for the derivatives of the interpolant are studied as well.

In Section 6, a comparison to the approach persued in [Lem95] is presented; this is based on interpolating the support function of a set-valued map, thus generating an interpolating set-valued map. Finally, the numerical results are gathered in the last section, showing that the directed sets are indeed a convenient tool for performing interpolation with higher polynomial degree, even for the more general Hermite interpolation problem.

We deliberately make use of the term "Kergin interpolation" and its notation to suggest that the presented approach may easily be extended to the scope of multivariate interpolation.

2 Directed Sets

2.1 Preliminaries

In this introductory subsection, the notation will be fixed and basic definitions will be presented.

Denote by $\|\cdot\|$ the Euclidean norm in $\mathbb{R}^n$, let $B_r(\mathrm{m})$ be the corresponding closed ball in $\mathbb{R}^n$ with radius r and center $m \in \mathbb{R}^n$ and $S_{n-1} \subset \mathbb{R}^n$ the unit sphere. The class of all non-empty convex compact sets in $\mathbb{R}^n$ is called $\mathcal{C}(\mathbb{R}^n)$. The support function $\delta^*(\cdot, A)$ of a set $A \in \mathcal{C}(\mathbb{R}^n)$ is defined in $\mathbb{R}^n$ as

$$\delta^*(l, A) := \max_{a \in A} \langle l, a \rangle \tag{1}$$

We leave out intentionally a review of the properties of the support function (cf. [Roc72], [Sch93]) assuming these to be well-known to the reader.

For any $l \in \mathbb{R}^n$ and $A \in \mathcal{C}(\mathbb{R}^n)$, we denote with

$$Y(l, A) = \{a \in A \quad | \quad \langle l, a \rangle = \delta^*(l, A)\} \tag{2}$$

the *supporting face* of A in the direction l. It equals the subdifferential $\partial\delta^*(l, A)$ of the support function. An element from $Y(l, A)$ will be denoted by $y(l, A)$ or, alternatively, in the more compact fashion y_A^l.

We consider the usual arithmetic operations together with the order relation for $A, B \in \mathcal{C}(\mathbb{R}^n)$, $\lambda \in \mathbb{R}$: the *Minkowski addition*

$$A + B := \{a + b \ | \ a \in A, b \in B\}, \tag{3}$$

multiplication by a real scalar

$$\lambda \cdot A := \{\lambda \cdot a \ | \ a \in A\}$$

and the order relation by inclusion

$$A \geq B \iff A \supseteq B.$$

(cf. e.g. [DKRV97]). For the particular case as for $\lambda = -1$, the notation $\ominus A$ is also often used. The *geometric/Pontryagin's difference* in [Had50, Pon67] is defined as

$$A \overset{*}{-} B := \bigcap_{l \in S_{n-1}} \{x \in \mathbb{R}^n \ | \ \langle l, x \rangle \leq \delta^*(l, A) - \delta^*(l, B)\}$$

which might be empty.

We denote by $\mathrm{d_H}\big(A, B\big)$ the *Hausdorff distance* of the two sets and by $\mathrm{d_D}\big(A, B\big)$ the correesponding *Demyanov distance*, i.e.

$$\begin{aligned} \mathrm{d_H}\big(A, B\big) &= \min\{\varepsilon > 0 \ : \ A \subset B + \varepsilon B_1(0), \ B \subset A + \varepsilon B_1(0)\}, \\ \mathrm{d_D}\big(A, B\big) &= \sup_{l \in S_{n-1}} \mathrm{d_H}\big(Y(l, A), Y(l, B)\big), \end{aligned}$$

cf. [RA92] for the original definition of the Demyanov distance and [Per07, Proposition 2.4.5].

2.2 Definition of Directed Sets

At this stage, basic facts concerning the directed sets introduced in [BF01a, BF01b] are briefly recalled. A directed set $\overrightarrow{A}$ is parametrised by directions $l \in S_{n-1}$ and consists of two components: a continuous function $a_n(l)$ and a $(n-1)$-dimensional uniformly bounded directed set function, $\overrightarrow{A_{n-1}(l)}$.

To motivate the meaning of those components and the embedding, a short discussion of projections and reprojections for hyperplanes is necessary. Let $a(\cdot)$ be a function from S_{n-1} into $\mathbb{R}$. For $l \in S_{n-1}$, $\mathcal{H}_a^l$ denotes the hyperplane

$$\mathcal{H}_a^l := \{x \in \mathbb{R}^n \mid \langle l, x\rangle = a(l)\}. \tag{4}$$

Being $\mathcal{H}_a^l$ and $\mathbb{R}^{n-1}$ isomorph for each $l \in S_{n-1}$, we introduce the affine function (shortly called *projection*)

$$\Pi_a^l : \mathcal{H}_a^l \longrightarrow \mathbb{R}^{n-1} \tag{5}$$

whose corresponding linear function is the isomorphic projection from $\mathcal{H}_0^l$ onto $\mathbb{R}^{n-1}$ (cf. [BF01a, BF01c, Per03]). The above linear function generates an (affine) *re-projection*

$${}^*\Pi_a^l : \mathbb{R}^{n-1} \longrightarrow \mathcal{H}_a^l \tag{6}$$

with $(\Pi_a^l \circ {}^*\Pi_a^l)(x) = x$ for all $x \in \mathcal{H}_a^l$.

For a directed set, the hyperplane $\mathcal{H}_a^l$ is fixed by $a(l) = a_n(l)$ and contains the re-projection of the visualisation of $\overrightarrow{A_{n-1}(l)}$. This image forms the boundary part of the visualised $\overrightarrow{A}$ in direction $l \in S_{n-1}$. For an embedded convex compact set C, the hyperplane $\mathcal{H}_{a_n}^l$ is determined by the value of its support function $\delta^*(\cdot, C)$ in direction l, whereas $\overrightarrow{A_{n-1}(l)}$ is the embedded projection of its supporting face $Y(l, C)$ (seen as $(n-1)$-dimensional set) into $\overrightarrow{\mathcal{D}}^{n-1}$.

The definition of a directed set is given recursively with respect to its dimension $n \in \mathbb{N}$.

Definition 2.1 *Consider $n \in \mathbb{N}$ and denote with $\overrightarrow{\mathcal{D}}^n$ the space of the directed sets of dimension n. A directed set of dimension $\mathbf{n = 1}$ is given by the expression*

$$\overrightarrow{A} := (a_1(l))_{l \in S_0} = (a_1(-1), a_1(+1))$$

for a function $a_1(\cdot) : S_0 \longrightarrow \mathbb{R}$. The norm of the one-dimensional $\overrightarrow{A}$ is defined as

$$\| \overrightarrow{A} \|_1 := \max_{l \in S_0} |a_1(l)| = \max\{|a_1(-1)|, |a_1(+1)|\}.$$

For higher dimensions $\boldsymbol{n \geq 2}$, a directed set $\overrightarrow{A} \in \overrightarrow{\mathcal{D}}^n$ is defined by a function

$$\begin{aligned} \overrightarrow{A} : S_{n-1} &\longrightarrow \overrightarrow{\mathcal{D}}^{n-1} \times \mathbb{R} \\ l &\mapsto (\overrightarrow{A_{n-1}(l)}, a_n(l)) \end{aligned}$$

Here, the second component $a_n(\cdot) : S_{n-1} \to \mathbb{R}$ is continuous and the first component $\overrightarrow{A_{n-1}(\cdot)} : S_{n-1} \to \overrightarrow{\mathcal{D}}^{n-1}$ has to be uniformly bounded with regard to the norm $\| \cdot \|_{n-1}$. The norm in $\overrightarrow{\mathcal{D}}^n$ is defined recursively as

$$\| \overrightarrow{A} \|_n := \max\{\sup_{l \in S_{n-1}} \|\overrightarrow{A_{n-1}(l)}\|_{n-1}, \max_{l \in S_{n-1}} |a_n(l)|\}. \tag{7}$$

We remark that for denoting a directed set $\overrightarrow{A} \in \overrightarrow{\mathcal{D}}^n$ the compact form

$$\left(\overrightarrow{A}^{\,l}_{n-1}, a^l_n\right)_{l\in S_{n-1}} \tag{8}$$

will be also often used. Notice that for $n = 1$ only the right-hand component is to be considered. Moreover, when the dimension n appears clear from the context, we drop the subscript in (7).

The above definition is motivated by the fact that the supporting face of each convex compact set $C \in \mathcal{C}(\mathbb{R}^n)$ in direction $l \in S_{n-1}$ lies on the hyperplane $\mathcal{H}^l_{\delta^*(\cdot,l)}$ given by the support function in this direction. To enable a recursive approach, the support function is saved separately from the supporting face and the latter is seen as a $(n-1)$-dimensional set.

The space $\overrightarrow{\mathcal{D}}^n$ establishes an important tool in within the work. In fact, convex compact sets can be embedded into the Banach space of the directed sets which establishes means for set arithmetics, visualisation and differentiation of corresponding set-valued maps. Of course, the embedding is also recursively defined. For further references on other possible embeddings and related articles see [BF01a, BF01b]. Concerning further details on the computation of the embedding one may refer to [Per03, Chapter 3 & 4].

Definition 2.2 *The embedding of $\mathcal{C}(\mathbb{R}^n)$ into $\overrightarrow{\mathcal{D}}^n$*

$$J_n : \mathcal{C}(\mathbb{R}^n) \longrightarrow \overrightarrow{\mathcal{D}}^n \tag{9}$$

is given by

$$J_n(A) = \begin{cases} \big(\delta^*(l,A)\big)_{l\in S_0} & \text{for } n = 1 \\ \Big(J_{n-1}\big(\Pi^l_{\delta^*(\cdot,A)}(Y(l,A)\big), \delta^*(l,A)\Big)_{l\in S_{n-1}} & \text{for } n \geq 2. \end{cases}$$

The operations of a real vector space are introduced component-wise in $\overrightarrow{\mathcal{D}}^n$.

Definition 2.3 *For $\overrightarrow{A} = \left(\overrightarrow{A}^{\,l}_{n-1}, a^l_n\right)_{l\in S_{n-1}}$, $\overrightarrow{B} = \left(\overrightarrow{B}^{\,l}_{n-1}, b^l_n\right)_{l\in S_{n-1}} \in \overrightarrow{\mathcal{D}}^n$ and $\lambda, \mu \in \mathbb{R}$, the operations are defined recursively:*

$$\lambda \cdot \overrightarrow{A} + \mu \cdot \overrightarrow{B} := \left(\lambda \cdot \overrightarrow{A}^{\,l}_{n-1} + \mu \cdot \overrightarrow{B}^{\,l}_{n-1}, \lambda\, a^l_n + \mu\, b^l_n\right)_{l\in S_{n-1}}$$

Notice that the first component of a directed set is not present for $n = 1$.

The definition of the directed sets, of the embedding of real intervals and of the arithmetic operations for the dimension $n = 1$ coincide with the ones for generalised/directed intervals as in [Kau80, Mar95].

2.3 Properties of Directed Sets

Endowed with the above operations, the space $\overrightarrow{\mathcal{D}}^n$ enjoys remarkable properties which are portrayed in [BF01a]. Above all, $\overrightarrow{\mathcal{D}}^n$ builds a Banach space (see [BF01a, Theorem 3.9]). Since we are basically interested in embedded elements of $\mathcal{C}(\mathbb{R}^n)$ (along with their difference and visualisation), we restrict our attention

to the Banach space consisting of the closure of the linear hull $\overrightarrow{\mathcal{C}}^n$ of $J_n(\mathcal{C}(\mathbb{R}^n))$ with respect to the norm in Definition 2.1.

The embedding in Definition 2.2 preserves the Minkowski-addition as well as the multiplication with a non-negative scalar as shown in [BF01a, Theorem 4.17].

Proposition 2.4 *Let A and B be in $\mathcal{C}(\mathbb{R}^n)$. Furthermore, consider real scalars $\lambda \geq 0$ and $\mu \geq 0$. Then the following equality holds:*

$$J_n(\lambda \cdot A + \mu \cdot B) = \lambda \cdot J_n(A) + \mu \cdot J_n(B)$$

The results of the interpolation performed in the numerical applications will be visualised in Section 7. Therefore, we now recall basic notion concerning the visalisation of directed sets; for more details, the reader may refer to [BF01b]. The visualisation of a directed set $\overrightarrow{A} \in \overrightarrow{\mathcal{C}}^n$ consists of three parts: the *convex part*

$$P_n(\overrightarrow{A}) := \bigcap_{l \in S_{n-1}} \{x \in \mathbb{R}^n \mid \langle l, x \rangle \leq a_n(l)\}, \tag{10}$$

the *concave part*

$$N_n(\overrightarrow{A}) := \ominus \bigcap_{l \in S_{n-1}} \{x \in \mathbb{R}^n \mid \langle l, x \rangle \leq -a_n(l)\}, \tag{11}$$

and the (non-convex) *mixed-type part*

$$M_n(\overrightarrow{A}) := B_n(\overrightarrow{A}) \setminus (\partial P_n(\overrightarrow{A}) \cup \partial N_n(\overrightarrow{A})). \tag{12}$$

Here, $B_n(\overrightarrow{A})$ is the *boundary part* given by

$$B_n(\overrightarrow{A}) := \begin{cases} \partial P_1(\overrightarrow{A}) \cup \partial N_1(\overrightarrow{A}) = \{-a_1(-1), a_1(+1)\}, & \text{if } n = 1, \\ \bigcup_{l \in S_{n-1}} {}^*\Pi^l_{a_n}(V_{n-1}(\overrightarrow{A_{n-1}(l)})), & \text{if } n \geq 2. \end{cases} \tag{13}$$

The *visualisation* is defined as the union

$$V_n(\overrightarrow{A}) := P_n(\overrightarrow{A}) \cup N_n(\overrightarrow{A}) \cup M_n(\overrightarrow{A}). \tag{14}$$

For each boundary point $x \in B_n(\overrightarrow{A})$, the *orientation bundle* denotes a set of unit directions with

$$\mathcal{O}_1(x, \overrightarrow{A}) := \begin{cases} \{-1\}, & \text{if } \overrightarrow{A} = \pm J_1([a,b]),\ a < b \text{ and } x = \pm a, \\ \{+1\}, & \text{if } \overrightarrow{A} = \pm J_1([a,b]),\ a < b \text{ and } x = \pm b, \\ \{\pm 1\}, & \text{if } \overrightarrow{A} = J_1(\{a\}),\ a = b \text{ and } x = a, \end{cases} \tag{15}$$

$$\mathcal{O}_n(x, \overrightarrow{A}) := \{l \in S_{n-1} : x \in {}^*\Pi^l_{a_n}(V_{n-1}(\overrightarrow{A_{n-1}(l)}))\}, \text{ if } n \geq 2. \tag{16}$$

At this stage some useful properties of the visualisation are presented. The following proposition shows that the visualisation of an embedded convex set $\overrightarrow{A}$ equals the set itself and explains how its inverse $-\overrightarrow{A}$ is visualised. Hereby, each boundary point of $\overrightarrow{A}$ is inverted, but keeps its orientation bundle.

Proposition 2.5
(i) For any embedded directed set $\overrightarrow{A} = J_n(A)$ *one has the following formulas for the visualisation:*

$$V_n(\overrightarrow{A}) = P_n(\overrightarrow{A}) \equiv A, \quad B_n(\overrightarrow{A}) = \partial A, \quad M_n(\overrightarrow{A}) = \emptyset \tag{17}$$

In particular, one obtains for the negative part and the orientation bundle:

$$\mathcal{O}_n(x, \overrightarrow{A}) = \{l \in S_{n-1} : x \in Y(l, A)\}, \quad N_n(\overrightarrow{A}) = \begin{cases} \{x\}, & \text{if} \quad A = \{x\}, \\ \emptyset & \text{otherwise.} \end{cases} \tag{18}$$

since each boundary point x *from* A *is an element of a suitable supporting face* $Y(l, A)$.
(ii) The parts of the visualisation of the inverse of a set $\overrightarrow{A} \in \overrightarrow{\mathcal{D}}^n$ *equal to:*

$$V_n(-\overrightarrow{A}) = \ominus V_n(\overrightarrow{A}), \quad B_n(-\overrightarrow{A}) = \ominus B_n(\overrightarrow{A}),$$
$$P_n(-\overrightarrow{A}) = \ominus N_n(\overrightarrow{A}), \quad N_n(-\overrightarrow{A}) = \ominus P_n(\overrightarrow{A}), \quad M_n(-\overrightarrow{A}) = \ominus M_n(\overrightarrow{A}).$$

Furthermore, $\mathcal{O}_n(-x, -\overrightarrow{A}) = \mathcal{O}_n(x, \overrightarrow{A})$ *for all* $x \in B_n(\overrightarrow{A})$.

Proof: (i) See [BF01b, Theorem 3.8 (i),(ii)]. The formula for the orientation bundle follows as in the proof of [BF01b, Proposition 3.8].
(ii) Follows immediately from the definitions, [BF01b, Proposition 2.5 (iv)] and [BF01b, Proposition 3.16]. ■

The difference of two embedded sets in $\mathcal{C}(\mathbb{R}^n)$ includes in its visualisation the geometric difference of the two sets.

Proposition 2.6 *Let* $\overrightarrow{A} = J_n(A)$, $\overrightarrow{B} = J_n(B)$ *for given* $A, B \in \mathcal{C}(\mathbb{R}^n)$. *Then,*

$$P_n(\overrightarrow{A} - \overrightarrow{B}) = A \overset{*}{-} B, \quad N_n(\overrightarrow{A} - \overrightarrow{B}) = \ominus(B \overset{*}{-} A) \quad \text{and} \quad V_n(\overrightarrow{A} - \overrightarrow{B}) \neq \emptyset.$$

Proof: Cf. [BF01b, Proposition 3.10] which also includes a more complex formula for the mixed-type part. ■

The visualisation (and, in particular, the boundary part) of a directed set is always non-empty: either the convex or concave part are non-empty (except for the degenerate case as for a point) or, if both are empty, the mixed-type part is non-empty (see [BF01b, Proposition 3.4]).

3 Derivatives

The images of convex-valued set-valued maps defined on $I = [t_0, T] \subset \mathbb{R}$ are embedded into the Banach space $\overrightarrow{\mathcal{D}}^n$.

Definition 3.1 *Let $F : I \Rightarrow \mathbb{R}^n$ be a convex-valued function, i.e. $F(t) \in \mathcal{C}(\mathbb{R}^n)$ for all $t \in I$. The embedded function $\overrightarrow{F}$ is given by the composition*

$$\overrightarrow{F} := J_n \circ F. \tag{19}$$

The usual notion of differentiability of functions having values in Banach spaces will be applied to embedded convex-valued maps as in [BF01c].

Definition 3.2 *A function $\overrightarrow{F} : I \to \overrightarrow{\mathcal{D}}^n$ is differentiable in $t \in I$, if the following limit exists:*

$$\mathrm{D}\,\overrightarrow{F}\,(t) := \lim_{\substack{h \to 0 \\ t+h \in I}} \frac{\overrightarrow{F}\,(t+h) - \overrightarrow{F}\,(t)}{h} \tag{20}$$

The directed set $\mathrm{D}\,\overrightarrow{F}\,(t)$ is called the derivative of $\overrightarrow{F}$ at t. The derivatives $\mathrm{D}^k\,\overrightarrow{F}$ of higher order $k \geq 2$ are defined recursively in the usual way. A convex-valued function $F : I \Rightarrow \mathbb{R}^n$ is said to be directed differentiable in t, if its embedding $\overrightarrow{F} := J_n \circ F$ is differentiable in this point.

As has been delineated in [BF01a, Per03], $\overrightarrow{F}\,(t)$ can be described alternatively as a vector of real-valued functions.

With the notation

$$\overrightarrow{F}\,(t) = \left(\overrightarrow{F}^{\,l}_{n-1}(t), f^l_n(t) \right)_{l \in S_{n-1}} \tag{21}$$

resembling (8), we state the differentiability formula for the components of a directed set function. The norm in Definition 2.1 demands intrinsically a certain uniformity within the limit (20) with respect to the parameter $l \in S_{n-1}$ for the set function (21).

Proposition 3.3 *If the map $\overrightarrow{F} : I \longrightarrow \overrightarrow{\mathcal{D}}^n$ is differentiable in $t \in I$, then both components are differentiable in t uniformly in $l \in S_{n-1}$ and*

$$\mathrm{D}\,\overrightarrow{F}\,(t) = \left(\mathrm{D}\,\overrightarrow{F}^{\,l}_{n-1}(t), \mathrm{D}\,f^l_n(t) \right)_{l \in S_{n-1}} \tag{22}$$

holds.

Proof: Recalling Definition 3.2 of the directed derivative, the limit

$$\mathrm{D}\,\overrightarrow{F}\,(t) := \lim_{\substack{h \to 0 \\ t+h \in I}} \frac{\overrightarrow{F}\,(t+h) - \overrightarrow{F}\,(t)}{h}$$

becomes

$$\lim_{\substack{h \to 0 \\ t+h \in I}} \left(\frac{\overrightarrow{F}^{\,l}_{n-1}(t+h) - \overrightarrow{F}^{\,l}_{n-1}(t)}{h}, \frac{f^l_n(t+h) - f^l_n(t)}{h} \right)_{l \in S_{n-1}}. \tag{23}$$

The limit (23) above corresponds to the limit of both components uniformly in $l \in S_{n-1}$ as the norm (7) enforces. Hence, the two components in

$$\left(\lim_{\substack{h \to 0 \\ t+h \in I}} \frac{\overrightarrow{F}^{\,l}_{\,n-1}(t+h) - \overrightarrow{F}^{\,l}_{\,n-1}(t)}{h}, \lim_{\substack{h \to 0 \\ t+h \in I}} \frac{f_n^l(t+h) - f_n^l(t)}{h} \right)_{l \in S_{n-1}} \tag{24}$$

converge uniformly in $l \in S_{n-1}$ and the assertion follows. ■

From the proof above, we understand that the uniformly differentiability of both components implies the directed differentiability of the map $\overrightarrow{F}$. We now present a central criterion for the directed differentiability of a convex-valued function (refer to [Per07, Theorem 3.2.2]) that depends only on the differentiability of the support function of the supporting face.

Proposition 3.4 (characterisation of smoothness) *The convex-valued map $F(\cdot)$ is directed differentiable in $t \in I$, if and only if the support function $\delta^*(\eta, Y\big(l, F(\cdot)\big))$ is differentiable in t in the classical sense uniformly in both arguments l and $\eta \in S_{n-1}$.*

Directed differentiability implies the smoothness of $t \mapsto \delta^*(l, F(t))$ uniformly in $l \in S_{n-1}$ which is very natural in the study of numerical methods for set-valued quadrature methods (cf. [DF90, Vel89a, BL94b]), in the study of set-valued Runge-Kutta methods (cf. [DF89, Vel89b, Vel92, BL94a, BL94b]) and in set-valued interpolation (cf. [DF90, Lem95]).

Corollary 3.5 *Suppose the convex-valued map $F(\cdot)$ is directed differentiable in $t \in I$. Then, the support function $\delta^*(l, F(\cdot))$ is differentiable in t in the classical sense uniformly in $l \in S_{n-1}$.*

Proof: Since $\delta^*(l, Y(l, F(\cdot))) = \delta^*(l, F(\cdot))$, Proposition 3.4 can be applied. ■

4 Set-Valued Divided Differences

In the following, let $I = [t_0, T]$ be a compact interval with $t_0 < T$. By convention, $\Theta \subset I$ will denote a *k-grid* of $k+1$ points $(\theta_0, \ldots, \theta_k)$, $k \in \mathbb{N}_0$, and Θ^j the sub-grid of the first $j+1$ elements of Θ, i.e. $(\theta_0, \ldots, \theta_j)$. $\Theta \setminus \Theta^j$ is the complementary grid $(\theta_{j+1}, \ldots, \theta_k)$ of Θ^j in Θ.

For any map $\overrightarrow{F} : \mathbb{R} \to \overrightarrow{\mathcal{D}}^n$, its divided difference of order j with respect to the k-grid Θ with pairwise disjoint nodes θ_i, $i = 0, \ldots, k$, is recursively defined in the usual manner (see e.g. [Dav75]) as in the following equations

$$\overrightarrow{F}[\theta_i] := \overrightarrow{F}(\theta_i), \tag{25}$$

$$\overrightarrow{F}[\theta_i, \theta_{i+1}, \ldots, \theta_{i+j}] := \frac{\overrightarrow{F}[\theta_{i+1}, \ldots, \theta_{i+j}] - \overrightarrow{F}[\theta_i, \ldots, \theta_{i+j-1}]}{\theta_{i+j} - \theta_i} \tag{26}$$

for $i = 0, \ldots, k-j$ in (25)–(26) with $j = 0$ in (25) resp. $j = 1, \ldots, k$ in (26).

The following lemma is meant to highlight the component-wise representation of the divided differences defined in (25)–(26) in the spirit of (21).

Lemma 4.1 *Let $\overrightarrow{F} : I \to \overrightarrow{\mathcal{D}}^n$ and $\Theta \subset I$ be a k-grid. Then, the divided difference $\overrightarrow{F}[\Theta]$ has the following component-wise representation:*

$$\overrightarrow{F}[\Theta] = \left(\overrightarrow{F}^l_{n-1}[\Theta], f^l_n[\Theta]\right)_{l \in S_{n-1}}$$

Proof: We proceed per induction on the order j of the divided difference. For $j = 0$ and $i = 0, \ldots, k$, (25) yields trivially with $\Theta = (\theta_i)$:

$$\overrightarrow{F}[\Theta] = \overrightarrow{F}(\theta_i) = \left(\overrightarrow{F}^l_{n-1}(\theta_i), f^l_n(\theta_i)\right)_{l \in S_{n-1}} = \left(\overrightarrow{F}^l_{n-1}[\Theta], f^l_n[\Theta]\right)_{l \in S_{n-1}}$$

For $j \geq 1$ and $i = 0, \ldots, k-j$, the recursive setting (26) applied to the j-grid $\Theta = (\theta_i, \theta_{i+1}, \ldots, \theta_{i+j})$ can be rewritten as

$$\overrightarrow{F}[\Theta^j] = \frac{\overrightarrow{F}[\Theta^j \setminus \Theta^0] - \overrightarrow{F}[\Theta^{j-1}]}{\theta_{i+j} - \theta_i} .$$

The inductive hypothesis and the operations in $\overrightarrow{\mathcal{D}}^n$ finally yield

$$\begin{aligned}
\overrightarrow{F}[\Theta^j] &= \frac{\left(\overrightarrow{F}^l_{n-1}[\Theta^j \setminus \Theta^0], f^l_n[\Theta^j \setminus \Theta^0]\right)_{l \in S_{n-1}} - \left(\overrightarrow{F}^l_{n-1}[\Theta^{j-1}], f^l_n[\Theta^{j-1}]\right)_{l \in S_{n-1}}}{\theta_{i+j} - \theta_i} \\
&= \left(\frac{\overrightarrow{F}^l_{n-1}[\Theta^j \setminus \Theta^0] - \overrightarrow{F}^l_{n-1}[\Theta^{j-1}]}{\theta_{i+j} - \theta_i}, \frac{f^l_n[\Theta^j \setminus \Theta^0] - f^l_n[\Theta^{j-1}]}{\theta_{i+j} - \theta_i}\right)_{l \in S_{n-1}} \\
&= (\overrightarrow{F}^l_{n-1}[\Theta^j], f^l_n[\Theta^j])_{l \in S_{n-1}} .
\end{aligned}$$

■

4.1 Hermite-Genocchi Formula

We state and prove a central result concerning the representation of the divided differences. In the case of a k-grid of pairwise disjoint points one has the equivalence between the recursive definition given in (25)–(26) and a representation through means of a Bochner integral involving a certain normalised spline.

Theorem 4.2 *Let $\Theta = (\theta_0, \ldots, \theta_k) \subset I$ be a k-grid consisting of pairwise disjoint points. If $\overrightarrow{F} : I \to \overrightarrow{\mathcal{D}}^n$ is k-times continuously directed-differentiable, then*

$$\overrightarrow{F}\,[\Theta] = \frac{1}{k!} \int_I \mathrm{M}(t|\Theta)\, \mathrm{D}^k \overrightarrow{F}\,(t)\ \mathrm{d}t \tag{27}$$

Proof: Cf. [Per07, Theorem 4.3.2] ■

The Hermite-Genocchi Formula in (27) deserves some further comments. First of all, the B-spline $\mathrm{M}(\cdot|\Theta)$ appears in Equation (27). In particular, the function $\mathrm{M}(\cdot|\Theta)$ is the normalised B-spline with knots Θ and

$$\int_I \mathrm{M}(t|\Theta)\, \mathrm{d}t = 1 \tag{28}$$

(see e.g. [de 01] or [PBP02]). Hereby, $k \in \mathbb{N}_0$ denotes the polynomial order of the spline and j denotes the index of the support $[\theta_j, \theta_{j+k}]$ of $\mathrm{M}(\cdot|\Theta)$. An extensive treatment of B-splines and its properties can be found e.g. in [CRE01, Chapter 6], [PBP02, Section 5.4 & 5.9], [de 76] or [de 01, Chapter IX]. Evidently, the support of the spline $\mathrm{M}(\cdot|\Theta)$ is included in the convex hull $\mathrm{co}(\Theta)$. Moreover, the integral on the right-hand in (27) is a Bochner integral, as introduced in [Boc33, HP74], because the right-hand side of (27) takes values in the Banach space $\overrightarrow{\mathcal{D}}^n$.

Due to Theorem 4.2, it is possible under certain assumptions to derive immediately some useful properties of divided differences by (27), in particular: the independence from the ordering of the knots in Θ; its continuity with respect to Θ; its meaning for collapsing points. Notice that the right-hand side of (27) could alternatively be rewritten as:

$$\int_{\Sigma_k} \mathrm{D}^k \overrightarrow{F}\Big(\theta_0 + (\theta_1 - \theta_0)\sigma_1 + \cdots + (\theta_k - \theta_0)\sigma_k\Big)\, \mathrm{d}\sigma$$

Hereby, Σ_k denotes the simplex $\Big\{(\sigma_1, \ldots, \sigma_k) \ \mid\ \sigma_1, \ldots, \sigma_k \geq 0\,,\ \sum_{i=1}^k \sigma_i \leq 1\Big\}$. For further details, one may see [Pet02, Fil04].

4.2 Estimates for the Divided Differences

Proposition 4.3 *Let $F : I \to \overrightarrow{\mathcal{D}}^n$ and $\Theta \subset I$ be a k-grid of different points. If F is k-times continuously directed-differentiable on I, then the estimate for the k-th divided difference is given by*

$$\big\|\overrightarrow{F}\,[\Theta]\big\| \leq \frac{1}{k!} \cdot \sup_{\theta \in [\theta_0, \theta_k]} \|\mathrm{D}^k \overrightarrow{F}\,(\theta)\|. \tag{29}$$

The reader should be aware that there are several possibilities for proving the statement. One short proof uses Theorem 4.2 (the Hermite-Genocchi formula) and the normalisation property (28). Another way would be an induction on the space dimension n. For $n = 1$, the statement is well-known for real-valued functions; for $n \geq 2$, Lemma 4.1 allows to study the two component functions separately. The argument for the second component is the same as for $n = 1$, the inductive assumption helps for the first component. This general approach is valid for many proofs in connection with directed sets.

The approach in the proof of [Per07, Theorem 4.3.2] consists in applying an induction per k (the order of the divided difference) and to use the recurrence formula for the derivative of the B-spline $N_j^k(\cdot)$ involved in the definition of $M(\cdot|\Theta)$ to establish the statement. In [DF90, Fil04] a different idea for the proofs has been persued instead. Basically, the scalarisation of the functions taking their values in Banach spaces by functionals allow to apply well-known results for real-valued functions. Finally, the separation of points by functionals is exploited to finish the proofs. In [Pet02] the restriction to finite-dimensional subspaces containing interpolation points plays a mayor role.

4.3 Coinciding Points

The limiting process, i.e. collapsing nodes in the k-grid of the interpolation data, is studied in the next proposition. It guarantees a continuity property of the divided differences generalising the real-valued result, e.g. in [DH03].

Proposition 4.4 *Assume $\overrightarrow{F} : I \longrightarrow \overrightarrow{\mathcal{D}}^n$ to be k-times continuously differentiable at $\theta \in I$. Furthermore, assume that the nodes θ_j, $j = 0, \ldots, k$, from the k-grids Θ in the following limit are all different. Then:*

$$\lim_{\substack{\theta_j \to \theta \\ 0 \le j \le k}} \overrightarrow{F}\,[\Theta] = \frac{1}{k!} \cdot \mathrm{D}^k \overrightarrow{F}\,(\theta) \tag{30}$$

Moreover, for any $\varepsilon > 0$ there exists a $\delta = \delta(\varepsilon) > 0$ depending on the continuity modulus of $\mathrm{D}^k \overrightarrow{F}\,(\cdot)$ such that for all k-grids Θ with different nodes θ_j, $j = 0, \ldots, k$, and $|\theta_j - \theta| \le \delta$ it follows that

$$\| \overrightarrow{F}\,[\Theta] - \frac{1}{k!} \cdot \mathrm{D}^k \overrightarrow{F}\,(\theta)\| \le \varepsilon. \tag{31}$$

Proof: We shall proceed by induction on n.

For $n = 1$, Proposition 3.3 shows that $f_1^l(\cdot)$ is k-times continuously differentiable in θ uniformly in $l \in S_{n-1}$. Since this function is real-valued, we already know that

$$\lim_{\substack{\theta_j \to \theta \\ 0 \le j \le k}} f_1^l[\Theta] = \frac{1}{k!} \cdot \frac{\mathrm{d}^k}{\mathrm{d}t^k} f_1^l(\theta).$$

Additionally, for each $l \in S_0$ there exists $\xi^l \in \mathrm{co}\{\theta_0, \ldots, \theta_k\}$ with

$$f_1^l[\Theta] = \frac{1}{k!} \cdot \frac{\mathrm{d}^k}{\mathrm{d}t^k} f_1^l(\xi^l).$$

Since the k-th derivative of $\overrightarrow{F}\,(\cdot)$ is continuous, there exists $\delta = \delta(\mathrm{D}^k \overrightarrow{F}\,) > 0$ such that for all $\theta_j \in [\theta - \delta, \theta + \delta] \cap I$ it follows that

$$|\frac{\mathrm{d}^k}{\mathrm{d}t^k} f_1^l(\xi^l) - \frac{\mathrm{d}^k}{\mathrm{d}t^k} f_1^l(\theta)| \le \|\mathrm{D}^k \overrightarrow{F}\,(\xi^l) - \mathrm{D}^k \overrightarrow{F}\,(\theta)\| \le k! \cdot \varepsilon, \tag{32}$$

because ξ^l is a convex combination of two nodes from Θ; δ depends only on $k! \cdot \varepsilon$ and on the continuity modulus of $\mathrm{D}^k \overrightarrow{F}\,(\cdot)$.

Now, let $n \geq 2$. Proposition 3.3 shows that $f_n^l(\cdot)$ and $\overrightarrow{F}^{\,l}_{n-1}(\cdot)$ are k-times continuously differentiable in θ uniformly in $l \in S_{n-1}$. Because of the inductive assumption and the fact that $f_n^l(\cdot)$ is real-valued it follows that

$$\lim_{\substack{\theta_j \to \theta \\ 0 \leq j \leq k}} \overrightarrow{F}^{\,l}_{n-1}[\Theta] = \frac{1}{k!} \cdot \mathrm{D}^k \overrightarrow{F}^{\,l}_{n-1}(\theta), \qquad \lim_{\substack{\theta_j \to \theta \\ 0 \leq j \leq k}} f_n^l[\Theta] = \frac{1}{k!} \cdot \frac{\mathrm{d}^k}{\mathrm{d}t^k} f_n^l(\theta).$$

The uniformity (with respect to $l \in S_{n-1}$) of the limits above is not yet evident. Moreover, the choice of $\delta(\mathrm{D}^k \overrightarrow{F}^{\,l}_{n-1})$ in (32) seems to depend on the continuity modulus of each function $\mathrm{D}^k \overrightarrow{F}^{\,l}_{n-1}(\cdot)$. Since

$$\begin{aligned} &\max\Big\{ \|\mathrm{D}^k \overrightarrow{F}^{\,l}_{n-1}(\theta_j) - \mathrm{D}^k \overrightarrow{F}^{\,l}_{n-1}(\theta)\|, \Big|\frac{\mathrm{d}^k}{\mathrm{d}t^k} f_n^l(\theta_j) - \frac{\mathrm{d}^k}{\mathrm{d}t^k} f_n^l(\theta)\Big| \Big\} \\ \leq &\|\mathrm{D}^k \overrightarrow{F}\,(\theta_j) - \mathrm{D}^k \overrightarrow{F}\,(\theta)\|, \end{aligned}$$

the inductive assumption can be exploited, $\delta(\mathrm{D}^k \overrightarrow{F}^{\,l}_{n-1})$ depends only on $k! \cdot \varepsilon$ and on the continuity modulus of $\mathrm{D}^k \overrightarrow{F}\,(\cdot)$ for each $l \in S_{n-1}$. For the second component function that is real-valued we can proceed as for $n = 1$; in fact, the argument with the continuity modulus can be repeated also here. Hence, the convergence is indeed uniformly in $l \in S_{n-1}$. Finally,

$$\begin{aligned} \lim_{\substack{\theta_j \to \theta \\ 0 \leq j \leq k}} \overrightarrow{F}\,[\Theta] &= \Big(\lim_{\substack{\theta_j \to \theta \\ 0 \leq j \leq k}} \overrightarrow{F}^{\,l}_{n-1}[\Theta], \lim_{\substack{\theta_j \to \theta \\ 0 \leq j \leq k}} f_n^l[\Theta] \Big)_{l \in S_{n-1}} \\ &= \Big(\frac{1}{k!} \cdot \mathrm{D}^k \overrightarrow{F}^{\,l}_{n-1}(\theta), \frac{1}{k!} \cdot \frac{\mathrm{d}^k}{\mathrm{d}t^k} f_n^l(\theta) \Big)_{l \in S_{n-1}} = \frac{1}{k!} \cdot \mathrm{D}^k \overrightarrow{F}\,(\theta). \end{aligned}$$

■

Remark 4.5 *For pairwise-disjoint grid points, we define the divided differences by means of* (25)–(26). *Equation* (30) *in Proposition 4.4 allows us to give a definition for the divided differences in the case that all grid points coincide. Otherwise, i.e. if only some grid points coincide, the recursive definition in* (26) *can still be applied for the definition. Moreover, Proposition 4.3 remains valid also in the case that all or some grid points coincide.*

At this stage all tools for introducing an interpolating map have been established.

5 The (Kergin) Interpolating Map

The following convention is introduced. Suppose that among the $k+1$ points $\theta_0, \ldots, \theta_k \in I = [t_0, T]$ only $m+1$, say $\widehat{\theta}_0, \ldots, \widehat{\theta}_m$, are distinct. Let θ_i occur in the list of points $\mu_i \geq 1$ times so that $k := \sum_{i=0}^{m} \mu_i - 1$, i.e.

$$\Theta := \Big(\theta_0, \theta_1, \ldots, \theta_k\Big) := \Big(\underbrace{\widehat{\theta}_0, \ldots, \widehat{\theta}_0}_{\mu_0}, \ldots, \underbrace{\widehat{\theta}_i, \ldots, \widehat{\theta}_i}_{\mu_i}, \ldots, \underbrace{\widehat{\theta}_m, \ldots, \widehat{\theta}_m}_{\mu_m}\Big) \tag{33}$$

Then, the (Hermite) interpolating map (that we will designate by $\mathcal{K}_\Theta \overrightarrow{F}$) for a $(\mu-1)$-times differentiable function $\overrightarrow{F} : I \to \overrightarrow{\mathcal{D}}^n$ with $\mu := \max_{i=0,\ldots,m} \mu_i$ determines the (Hermite) polynomial map, for which the interpolation conditions

$$\mathrm{D}^i\big(\mathcal{K}_\Theta \overrightarrow{F}\ \big)(\widehat{\theta}_j) = \mathrm{D}^i \overrightarrow{F}\,(\widehat{\theta}_j) \quad (i = 0, \ldots, \mu_j - 1, \quad j = 0, \ldots, m) \tag{34}$$

hold.

The interpolation property in the following proposition is well-known (cf. [Pre71, Theorems 4.3 and 5.2], [DF90], [Pet02, Theorem 1], and [Fil04, Theorem 5.7]) and generalises, cf. [DH03, Theorem 7.6], to the set-valued case. Hereby, the interpolation approach propagates to the components of the directed set function so that the interpolating map is always polynomial with respect to t.

Proposition 5.1 *Let $\Theta \subset I$ be the k-grid in* (33) *and $\overrightarrow{F} : I \longrightarrow \overrightarrow{\mathcal{D}}^n$ be $(\mu-1)$-times continuously differentiable in I with $\mu := \max_{i=0,\ldots,m} \mu_i$.*
Then, the polynomial map

$$\mathcal{K}_\Theta \overrightarrow{F} : I \to \overrightarrow{\mathcal{D}}^n$$

of degree less or equal to k interpolating F on the k-grid Θ with conditions (34)*, is given by*

$$\big(\mathcal{K}_\Theta \overrightarrow{F}\ \big)(t) := \sum_{j=0}^{k} \omega_\Theta^{j-1}(t) \cdot \overrightarrow{F}\,[\Theta^j]. \tag{35}$$

Hereby, $\omega_\Theta^{j-1}(t) = \prod_{i=0}^{j-1}(t - \theta_i)$, $j = 0, \ldots, k$. The map above exhibits the following component-wise representation:

$$\mathcal{K}_\Theta \overrightarrow{F} \equiv \Big(\mathcal{K}_\Theta \overrightarrow{F}^{\,l}_{n-1}, \mathcal{K}_\Theta f^l_n\Big)_{l \in S_{n-1}} \tag{36}$$

Proof: Denote $\mathcal{K}_\Theta \overrightarrow{F}\,(t)$ with $\overrightarrow{H}\,(t)$. First of all, Lemma 4.1 shows that

$$\overrightarrow{H}^{\,l}_{n-1}(t) = \sum_{j=0}^{k} \omega_\Theta^{j-1}(t) \cdot \overrightarrow{F}^{\,l}_{n-1}[\Theta^j] \tag{37}$$

and

$$h^l_n(t) = \sum_{j=0}^{k} \omega_\Theta^{j-1}(t) \cdot f^l_n[\Theta^j]. \tag{38}$$

Proposition 3.3 allows to rewrite the interpolation conditions in (34) as

$$\mathrm{D}^i\big(\overrightarrow{H}^{\,l}_{n-1}\big)(\widehat{\theta}_j) = \mathrm{D}^i\,\overrightarrow{F}^{\,l}_{n-1}(\widehat{\theta}_j), \quad \frac{\mathrm{d}^i}{\mathrm{d}t^i} h^l_n(\widehat{\theta}_j) = \frac{\mathrm{d}^i}{\mathrm{d}t^i} f^l_n(\widehat{\theta}_j)$$

for $i = 0, \ldots, m_j - 1$, $j = 0, \ldots, m$.

At this stage we proceed per induction on n.

$n = 1$: The uniqueness result for real-valued Hermite interpolation shows that $h^l_1 = K_\Theta f^l_1$.

Similarly, for $n \geq 2$ one may immediately show that $h^l_n = K_\Theta f^l_n$. The inductive assumption shows that $\overrightarrow{H}^{\,l}_{n-1} = \mathcal{K}_\Theta\,\overrightarrow{F}^{\,l}_{n-1}$. Hence, (36) follows from (37)–(38). ■

The term $\mathcal{K}_\Theta\,\overrightarrow{F}$ respectively $\mathcal{K}_\Theta\,\overrightarrow{F}^{\,l}_{n-1}$ is the Kergin interpolating map in a Banach space (i.e. $\overrightarrow{\mathcal{D}}^n$ respectively $\overrightarrow{\mathcal{D}}^{n-1}$; refer to [Pet02, Fil04]); $\mathcal{K}_\Theta f^l_n$ is the well-known real-valued (Kergin) interpolating map (see e.g. [Ker80]). The map in (35) is a polynomial with values in a Banach space in the sense of [Pre71, Section 2], [DF90, Definition 2] and [Fil04, Section 2].

After having introduced an interpolating map, we focus on deriving estimates for the interpolation error. We will designate by $\overrightarrow{\mathcal{R}}_\Theta$ the remainder term; it acts component-wise because of Proposition 5.1. Thus:

$$\overrightarrow{\mathcal{R}}_\Theta = \overrightarrow{F} - \mathcal{K}_\Theta\,\overrightarrow{F} = \Big(\overrightarrow{\mathcal{R}}^{\,l}_{\Theta,n-1}, r^l_{\Theta,n}\Big)_{l\in S_{n-1}}, \tag{39}$$

where

$$\overrightarrow{\mathcal{R}}^{\,l}_{\Theta,n-1} = \overrightarrow{F}^{\,l}_{n-1} - \mathcal{K}_\Theta\,\overrightarrow{F}^{\,l}_{n-1}, \quad r^l_{\Theta,n} = f^l_n - \mathcal{K}_\Theta f^l_n \quad (l \in S_{n-1}).$$

Variants of the following Proposition 5.2 are already known. The error representation presented in (41) is proved in [Fil04, Theorem 6.1] and used in [Fil04, Theorem 6.2] to show an error estimate for the more restrictive class of holomorphic functions. For an estimation with the modulus of smoothness for Lagrange interpolation and another embedding of $\mathcal{C}(\mathbb{R}^n)$ into a vector space under weaker smoothness assumptions, see [DF90, Corollary 3].

Proposition 5.2 *Let $\overrightarrow{F} : I \longrightarrow \overrightarrow{\mathcal{D}}^n$ be $(k+1)$-times continuously differentiable and $k = \big(\sum_{j=0}^m \mu_j\big) - 1$. Then the following error estimate holds for $t \in I$:*

$$\|\overrightarrow{\mathcal{R}}_\Theta(t)\| \leq \frac{1}{(k+1)!} \cdot \max_{\tau\in I} \|\mathrm{D}^{k+1}\,\overrightarrow{F}(\tau)\| \cdot \prod_{j=0}^m |t - \widehat{\theta}_j|^{\mu_j} \tag{40}$$

Proof: With $\overrightarrow{\mathcal{R}}_\Theta$ as in (39) one has as in [Pet02, Lemma 2]:

$$\overrightarrow{\mathcal{R}}_\Theta(t) = \omega^k_{(\Theta,t)}(t) \cdot \overrightarrow{F}\,[(\Theta,t)], \quad \omega^k_{(\Theta,t)}(t) = \prod_{j=0}^m (t - \widehat{\theta}_j)^{\mu_j} \tag{41}$$

Now, Proposition 4.3 together with Remark 4.5 yields the assertion. ■

The next two results represent generalisations of the real-valued case. Other error estimates known for real-valued functions could be transferred to $\overrightarrow{\mathcal{D}}^n$ in a similar manner. The first estimation (cf. [Kan74, Satz 3] for the real-valued case) provides an estimate for the interpolation error of the derivatives up to order $(k+1)$.

Lemma 5.3 *Let $\overrightarrow{F} : I \longrightarrow \overrightarrow{\mathcal{D}}^n$ be $(k+1)$-times continuously differentiable. Then, the following error estimate holds for $j = 0, \ldots, k+1$ and $t \in I$:*

$$\begin{aligned} &\|\mathrm{D}^j \overrightarrow{F}(t) - \mathrm{D}^j\big(\mathcal{K}_\Theta \overrightarrow{F}\big)(t)\| \\ \leq\ & \frac{1}{(k+1-j)!} \cdot \max_{\tau \in I} \|\mathrm{D}^{k+1} \overrightarrow{F}(\tau)\| \cdot \prod_{i=0}^{k-j} \max\big\{|t-\theta_i|, |t-\theta_{i+j}|\big\} \end{aligned}$$

Proof: We shall start with $n \geq 2$, since the real-valued case is known for $n = 1$, and set $\overrightarrow{H}(t) := \mathcal{K}_\Theta \overrightarrow{F}(t)$.

We begin with estimating the second component of $\overrightarrow{F} - \overrightarrow{H}$ by [Kan74, Satz 3]. Thus:

$$\begin{aligned} &|\frac{\mathrm{d}^j}{\mathrm{d}t^j} f_n^l(t) - \frac{\mathrm{d}^j}{\mathrm{d}t^j} h_n^l(t)| \\ &\leq \frac{1}{(k+1-j)!} \cdot \|\frac{\mathrm{d}^{k+1}}{\mathrm{d}t^{k+1}} f_n^l\|_\infty \cdot \prod_{i=0}^{k-j} \max\big\{|t-\theta_i|, |t-\theta_{i+j}|\big\} \end{aligned} \tag{42}$$

for $j = 0, \ldots, k+1$ and $l \in S_{n-1}$. Concerning the first component, one obtains with the inductive assumption:

$$\begin{aligned} &|\mathrm{D}^j \overrightarrow{F}_{n-1}^l(t) - \mathrm{D}^{k+1} \overrightarrow{H}_{n-1}^l(t)| \\ &\leq \frac{1}{(k+1-j)!} \cdot \|\mathrm{D}^{k+1} \overrightarrow{F}_{n-1}^l\|_\infty \cdot \prod_{i=0}^{k-j} \max\big\{|t-\theta_i|, |t-\theta_{i+j}|\big\}. \end{aligned} \tag{43}$$

Since the estimate

$$\max\Big\{\|\mathrm{D}^{k+1} \overrightarrow{F}_{n-1}^l\|_\infty, \Big\|\frac{\mathrm{d}^{k+1}}{\mathrm{d}t^{k+1}} f_n^l\Big\|_\infty\Big\} \leq \|\mathrm{D}^{k+1} \overrightarrow{F}\|_\infty$$

in (42)–(43) holds, the assertion follows. ■

Consider a fixed step-size $h = \frac{T-t_0}{N}$, $N \in \mathbb{N}$, and the knot-grid $\widehat{\theta}_i := t_0 + ih \in I = [t_0, T]$, $i = 0, \ldots, N$. Set

$$\Theta_i := (\underbrace{\widehat{\theta}_i, \ldots, \widehat{\theta}_i}_{\mu}, \underbrace{\widehat{\theta}_{i+1}, \ldots, \widehat{\theta}_{i+1}}_{\mu}),$$

$I_i := [\widehat{\theta}_i, \widehat{\theta}_{i+1}]$ and denote with $\overrightarrow{H}$ the piecewise defined map consisting of Hermite interpolating maps $\overrightarrow{H}_i$ on I_i for $i = 0, \ldots, N$ with polynomial order $2\mu - 1$, $\mu = \mu_0 = \mu_1$; thus: $m = 1$, $k = 2\mu - 1$ in (33) and

$$\mathcal{K}_{\Theta_i} \overrightarrow{F}_{|I_i} = \overrightarrow{H}_i\,.$$

Following the idea of the proof of [BSV68, Theorem 2], we formulate the following estimation for the set-valued piecewise Hermite interpolation.

Corollary 5.4 *Assume $\overrightarrow{F} : I \to \overrightarrow{\mathcal{D}}^n$ to be (2μ)-times continuously differentiable. Then, the following error estimate holds for the piecewise Hermite interpolation with polynomial order $2\mu - 1$ and step-size h defined above for $t \in I$ and derivatives of order $j = 0, \ldots, \mu - 1$:*

$$\|\mathrm{D}^j \overrightarrow{F}(t) - \mathrm{D}^j \overrightarrow{H}(t)\| \leq \frac{1}{(2\mu - j)!} \cdot \max_{\tau \in I} \|\mathrm{D}^{2\mu} \overrightarrow{F}(\tau)\| \cdot h^{2\mu - j} \tag{44}$$

Proof: Lemma 5.3 can be applied on I_i for $j = 0, \ldots, 2\mu$ yielding

$$\begin{aligned}
&\|\mathrm{D}^j \overrightarrow{F}(t) - \mathrm{D}^j \overrightarrow{H}(t)\| = \|\mathrm{D}^j \overrightarrow{F}(t) - \mathrm{D}^j \overrightarrow{H}_i(t)\| \\
&\leq \frac{1}{(2\mu - j)!} \cdot \max_{\tau \in I} \|\mathrm{D}^{2\mu} \overrightarrow{F}(\tau)\| \cdot \prod_{\nu=0}^{2\mu-j-1} \max\left\{|t - \theta_{i,\nu}|, |t - \theta_{i,\nu+j}|\right\} \\
&\leq \frac{1}{(2\mu - j)!} \cdot \max_{\tau \in I} \|\mathrm{D}^{2\mu} \overrightarrow{F}(\tau)\| \cdot h^{2\mu-j},
\end{aligned}$$

where

$$\theta_{i,\nu} = \begin{cases} \widehat{\theta}_i & \text{for } \nu = 0, \ldots, \mu - 1, \\ \widehat{\theta}_{i+1} & \text{for } \nu = \mu, \ldots, 2\mu - 1. \end{cases}$$

Notice that $\overrightarrow{H}$ is $(\mu - 1)$-times continuously differentiable on I, having the following conditions to hold for $i = 0, \ldots, N - 1$:

$$\mathrm{D}^j \overrightarrow{H}(\widehat{\theta}_i) = \mathrm{D}^j \overrightarrow{F}(\widehat{\theta}_i) \quad \text{and} \quad \mathrm{D}^j \overrightarrow{H}(\widehat{\theta}_{i+1}) = \mathrm{D}^j \overrightarrow{F}(\widehat{\theta}_{i+1}) \quad (j = 0, \ldots, \mu - 1)$$

Hence, the global estimation on I is valid only for $j = 0, \ldots, \mu - 1$. ■

6 Connections to Other Approaches

Consider $t \in I$ and the representation of the images of a convex-valued map $F : I \Longrightarrow \mathbb{R}^n$ through means of the support function:

$$F(t) = \bigcap_{l \in S_{n-1}} \big\{ x \in \mathbb{R}^n \ \mid \ \langle l, x \rangle \ \leq \ \delta^l(t) \big\} \tag{45}$$

Hereby, we set $\delta^l(t) := \delta^*(l, F(t))$ for simpleness of notation.

In [Lem95], polynomial interpolation of δ^l for every $l \in S_{n-1}$ underlies the following set-valued approximation of $F(t)$:

$$\big(\mathcal{L}_\Theta F\big)(t) := \bigcap_{l \in S_{n-1}} \big\{ x \in \mathbb{R}^n \ \mid \ \langle l, x \rangle \ \leq \ \big(\mathcal{K}_\Theta \delta^l\big)(t) \big\} \tag{46}$$

Notice that $\mathcal{L}_\Theta F$ may result in an empty set for some t; in fact, $l \mapsto \mathcal{K}_\Theta \delta^l(t)$ might not be convex and thus, may not be a support function of $\big(\mathcal{L}_\Theta F\big)(t)$.

Before discussing the connection to the approach with the directed sets, we notice that Proposition 5.1 holds true in particular for the embedding of any sufficiently smooth (in the directed sense) convex-valued map $F : I \Rightarrow \mathbb{R}^n$. The specialisation for this case yields as one component the (Kergin) interpolation of the support function as in [Lem95], but takes into account also lower-dimensional projections of support faces.

Corollary 6.1 *Consider $\Theta \subset I$ and μ as in Proposition 5.1. Let $F : I \Rightarrow \mathbb{R}^n$ be a convex-valued function and $\overrightarrow{F}$ denote its embedding. If F is assumed $(\mu - 1)$-times directed-differentiable, then the (Kergin) interpolating map equals*

$$\mathcal{K}_\Theta \, \overrightarrow{F} \ = \Big(\mathcal{K}_\Theta \, \overrightarrow{F}^{\,l}_{n-1}, \mathcal{K}_\Theta \, \delta^*(l, F(\cdot)) \Big)_{l \in S_{n-1}} \tag{47}$$

with $\overrightarrow{F}^{\,l}_{n-1}(t) = J_{n-1}\big(\Pi^l_{\delta^*(\cdot, F(t))}(Y(l, F(t))\big)$.

We underline the fact that the second component in (47) reads

$$\begin{aligned} \big(\mathcal{K}_\Theta \delta^l\big)(t) = \delta^l[\theta_0] &+ \Big(\delta^l[\theta_0, \theta_1]\Big) \cdot (t - \theta_0) \\ &+ \Big(\delta^l[\theta_0, \theta_1, \theta_2]\Big) \cdot (t - \theta_0)(t - \theta_1) + \ldots \\ &+ \Big(\delta^l[\theta_0, \ldots, \theta_k]\Big) \cdot (t - \theta_0)\,(t - \theta_1) \cdots (t - \theta_{k-2})\,(t - \theta_{k-1}) \end{aligned}$$

for every $l \in S_{n-1}$, i.e. coincides with the Newton form of the interpolating polynomial to $\delta^l(\cdot)$ with nodes Θ. By writing $\mathcal{K}_\Theta \delta^l$ in its Lagrange form and by sorting out the negative weights, we obtain

$$\big(\mathcal{K}_\Theta \delta^l\big)(t) = \sum_{j : \ell_j(t) \geq 0} \ell_j(t) \delta^l(\theta_j) - \sum_{j : \ell_j(t) < 0} |\ell_j(t)| \cdot \delta^l(\theta_j)$$

with the Lagrange polynomials

$$\ell_j(t) = \prod_{\substack{\nu = 0, \ldots, k \\ \nu \neq j}} \frac{t - \theta_\nu}{\theta_j - \theta_\nu}, \quad j = 0, \ldots, k.$$

It becomes hence evident that $\mathcal{L}_\Theta F$ corresponds to the geometric difference

$$\big(\mathcal{L}_\Theta F\big)(t) = C(t) \overset{*}{-} D(t) = P_n\big(J_n(C(t)) - J_n(D(t))\big),$$

where we have used the notation of Subsection 2.1 and 2.3 and have introduced the two set-valued maps

$$C(t) = \sum_{j:\ell_j(t)\geq 0} \ell_j(t)F(\theta_j) \quad \text{and} \quad D(t) = \sum_{j:\ell_j(t)<0} |\ell_j(t)| \cdot F(\theta_j) \in \mathcal{C}(\mathbb{R}^n).$$

As a consequence of (14) and Proposition 2.6, interpolation with the directed sets yields actually a "super-map" of the approach as in [Lem95], when visualising the values of the interpolating map. This fact is summarised in the following proposition.

Proposition 6.2 *Let $F : I \Rightarrow \mathbb{R}^n$ be a convex-valued function and assume that all conditions in Corollary 6.1 hold. Then:*

$$\big(\mathcal{L}_\Theta F\big)(t) = P_n\big(\big(\mathcal{K}_\Theta \overrightarrow{F}\ \big)(t)\big) \subseteq V_n\big(\big(\mathcal{K}_\Theta \overrightarrow{F}\ \big)(t)\big) \neq \emptyset \tag{48}$$

for every $t \in I$.

Since the convex part of a directed set may be empty, conditions on the set-valued map F are required in [Lem95, Corollary 2.5] to achieve non-emptiness of the images of the interpolating map $\mathcal{L}_\Theta F$. The following proposition recalls both these conditions and [Lem95, Lemma 2.6].

Proposition 6.3 *Let $\Theta = (\theta_0, \ldots, \theta_k) \subset I$ be a k-grid consisting of pairwise disjoint points and $F : I \Rightarrow \overrightarrow{\mathcal{D}}^n$ be a convex-valued map. For $t \in I$, set*

$$\varepsilon(t) := \sup_{l\in S_{n-1}} |\delta^l(t) - \big(\mathcal{K}_\Theta \delta^l\big)(t)|,$$
$$c(t) := \max_{l\in S_{n-1}} \big(\mathcal{K}_\Theta \delta^l\big)(t)$$

Then, the following error estimates hold for the two possible cases below:
(i) If $\delta^*(l, (\mathcal{L}_\Theta F)(t)) = K_\Theta \delta^l(t)$, then

$$\mathrm{d_H}\big(F(t), \big(\mathcal{L}_\Theta F\big)(t)\big) = \varepsilon(t).$$

(ii) Otherwise if $\delta^*(l, (\mathcal{L}_\Theta F)(t)) < K_\Theta \delta^l(t)$, then we assume additionally the existence of a ball $B_{r(t)}(m(t))$ with centre $m(t) \in \mathbb{R}^n$ and radius $r(t) > 0$ that is contained entirely in the image $F(t)$ as well as that the error fulfills $0 < \varepsilon(t) < r(t)$. Then,

$$\mathrm{d_H}\big(F(t), \big(\mathcal{L}_\Theta F\big)(t)\big) \leq \frac{2c(t)}{r(t) - \varepsilon(t)} \cdot \varepsilon(t).$$

Because of the conditions expressed above, the difference of the two support functions of $F(t)$ respectively of $\big(\mathcal{L}_\Theta F\big)(t)$ can be estimated through means of the difference $\delta^l(t) - \big(\mathcal{K}_\Theta \delta^l\big)(t)$; it also tells us that $\big(\mathcal{L}_\Theta F\big)(t)$ is non-empty.

We notice that in [Lem95] the support function $\delta^*(l, F(\cdot))$ of each image $F(t) \in \mathcal{C}(\mathbb{R}^n)$ is interpolated polynomially. Nevertheless, the interpolating map as a whole is not, in general, polynomial as a set-valued function (with respect to

the parameter t) like in the approach with directed sets. In the latter approach, the first component leading back to the supporting face is considered in view of Corollary 6.1 and interpolated as well. Since $\overrightarrow{\mathcal{D}}^n$ is a Banach space (which also offers a visualisation for all directed sets), the values of the interpolating function $\big(\mathcal{K}_\Theta \overrightarrow{F}\ \big)(t) = J_n(C(t)) - J_n(D(t))$ always have a non-empty visualisation by Proposition 2.6. Therefore, an interior ball condition as in (ii) of the above proposition is not necessary.

Remark 6.4 *Piecewise constant and linear set-valued interpolation (cf. [Vit79, Art89, Nik90a, Nik90b, Nik93, Mar93, MA96, MPSS96, Nik90a, Nik90b]) are special cases of the Kergin interpolation with directed sets as introduced in Section 5. For the embedded function $\overrightarrow{F}\ (t) = J_n(F(t))$ and a k-grid Θ with $k \leq 1$ different points, it follows that:*

$$\begin{aligned}\big(\mathcal{K}_\Theta \overrightarrow{F}\ \big)(t) &= \begin{cases} \overrightarrow{F}\ (\theta_0) & \text{if } k = 0, \\ \overrightarrow{F}\ (\theta_0) + (t-\theta_0) \cdot \frac{1}{\theta_1-\theta_0} \cdot \big(\overrightarrow{F}\ (\theta_1) - \overrightarrow{F}\ (\theta_0)\big) & \text{if } k = 1 \end{cases} \\ &= \begin{cases} J_n(F(\theta_0)) & \text{if } k = 0, \\ J_n\big(\big(\frac{\theta_1-t}{\theta_1-\theta_0} \cdot F(\theta_0) + \frac{t-\theta_0}{\theta_1-\theta_0} \cdot F(\theta_1)\big)\big) & \text{if } k = 1. \end{cases}\end{aligned}$$

In both cases, $k = 0, 1$, the interpolation of $\overrightarrow{F}\ (\cdot)$ coincides with the usual set-valued interpolation because of Proposition 2.5(i), i.e.

$$V_n\big(\big(\mathcal{K}_\Theta \overrightarrow{F}\ \big)(t)\big) = \big(\mathcal{L}_\Theta F\big)(t) = \begin{cases} F(\theta_0) & \text{if } k = 0, \\ \frac{\theta_1-t}{\theta_1-\theta_0} \cdot F(\theta_0) + \frac{t-\theta_0}{\theta_1-\theta_0} \cdot F(\theta_1) & \text{if } k = 1. \end{cases}$$

Clearly, $\big(\mathcal{K}_\Theta \delta^l\big)(t)$ is the support function of $\big(\mathcal{L}_\Theta F\big)(t)$ in these two cases.

7 Numerical Tests

The computations presented in this section aim to corroborate the theory shown so far; in particular, the interest is focused on the order of convergence. Similar computations for polynomial interpolation have been already performed with the aid of the software tool *SVUPI*, a *C++* collection of classes in [Per07].

In all the presented examples , the function F is sufficiently often directed-differentiable on the interval $[0, 1]$; this fact follows from easy calculations of the embedding. Furthermore, in Examples 7.2–7.4 the additional geometric conditions of Proposition 6.3(ii) are satisfied, especially the existence of an interior ball with a uniform radius for all images of the set-valued map F. As Proposition 5.2 demonstrates and Example 7.1 shows *inter alia*, no particular geometrical conditions on F have to be assumed for guaranteeing the order of convergence, since the visualisation is always non-empty for directed sets (cf. Proposition 6.2).

The computations are performed taking into account a discrete set of directions. The perturbation analysis with respect to the finite number of unit directions (instead of for all unit directions) is discussed in [Per07, Section 6.1]. The analysis profits from the equivalence between the norm in the space of directed sets and the Demyanov-distance, cf. [BF01a].

In the first four examples, the derivative at the boundary points are depicted. We shall also notice that the interpolating map actually matches F within plot precision.

Example 7.1 *We interpolate the set-valued map $F : [0, 1] \Longrightarrow \mathbb{R}^2$ given by $F(t) = t^5 \cdot [-1, 1]^2$. The unit square is scaled by a function with non-negative derivative, cf. left picture in Figure 1. Hence, $\mathrm{D}\overrightarrow{F}(t) = 5 \cdot t^4 \cdot J_2([-1, 1]^2)$; the values of the derivative consist of embedded convex sets with outer normals, cf. the middle respectively the right picture in the same figure. Incidentally,*

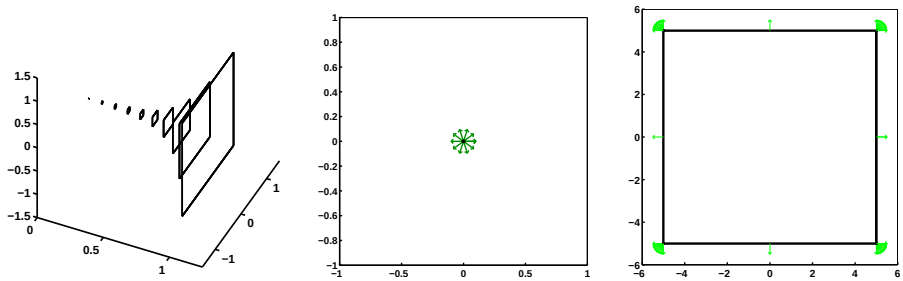

Figure 1: Funnel of $F(\cdot)$ and derivative data $D\overrightarrow{F}(0)$ and $D\overrightarrow{F}(1)$

notice that F violates the geometrical condition mentioned above, since there is no interior of $F(t)$ at time $t = 0$.
For the Hermite interpolation nodes $\Theta = (0, 1)$, $\mu_i = 2$, $i = 0, 1$, and the test points $\tau_i = \frac{i}{10}$, $i = 0, \ldots, 10$, we get the following error estimate for the Hermite interpolation polynomial $\overrightarrow{H_3}(\cdot)$ of degree 3:

$$\max_{i=0,\ldots,10} \|\overrightarrow{F}(\tau_i) - \overrightarrow{H_3}(\tau_i)\| = 0.0489$$

Example 7.2 *We interpolate the set-valued map* $F : [0,1] \Longrightarrow \mathbb{R}^2$ *given by* $F(t) = e^{-t} \cdot B(0,1)$*, cf. Figure 2. The scaling function for the Euclidean unit ball has negative derivative, so that the values* $\mathrm{D}\overrightarrow{F}(t) = -e^{-t} \cdot J_2(B(0,1))$ *of the derivative consist of inverses of embedded convex sets with inner normals, cf. the same figure. Nevertheless, the values of the interpolating polynomial have as visualisation only convex images. For the same Hermite interpolating*

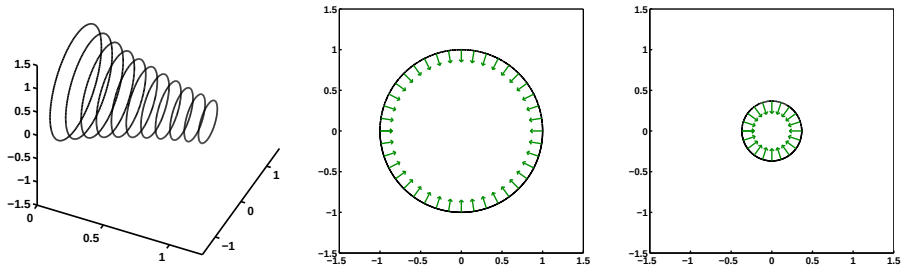

Figure 2: Funnel of $F(\cdot)$ and derivative data $D\overrightarrow{F}(0)$ and $D\overrightarrow{F}(1)$

polynomial and the test points τ_i *as in Example 7.1, we obtain the following error estimate:*

$$\max_{i=0,\ldots,10} \|\overrightarrow{F}(\tau_i) - \overrightarrow{H_3}(\tau_i)\| = 0.00161$$

Notice that, although the visualisations are concave, the overall result is convex. In the examples now following, attention is focused on the order of convergence.

Example 7.3 *The convex-valued function* F *(with its funnel and two function values depicted in Figure 3) to be interpolated reads:*

$$F : [0,1] \Longrightarrow \mathbb{R}^2 : t \mapsto e^t \cdot [-1,1]^2 + \frac{1}{2}e^{-t} \cdot B(0,1) \tag{49}$$

Passing on to the embedding, its expression reads:

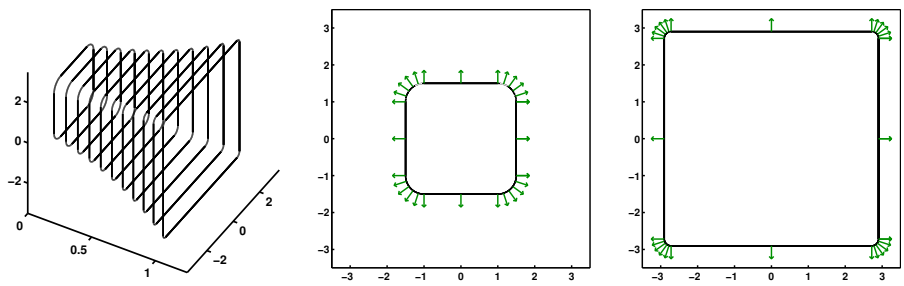

Figure 3: Funnel of $F(\cdot)$ and data $\overrightarrow{F}(0)$ and $\overrightarrow{F}(1)$

$$\overrightarrow{F}(t) = e^t \cdot J_2\big([-1,1]^2\big) + \frac{1}{2}e^{-t} \cdot J_2\big(B(0,1)\big),$$
$$D\overrightarrow{F}(t) = e^t \cdot J_2\big([-1,1]^2\big) - \frac{1}{2}e^{-t} \cdot J_2\big(B(0,1)\big)$$

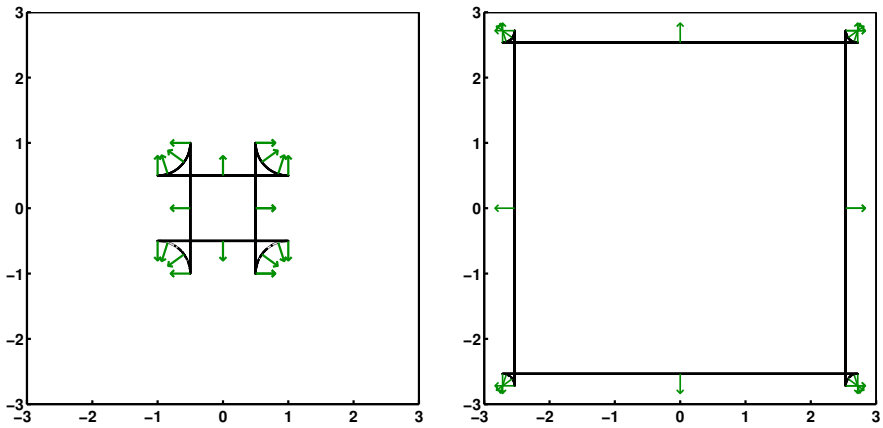

Figure 4: derivative data $D\overrightarrow{F}(0)$ and $D\overrightarrow{F}(1)$

As shown in Figure 4, the derivative involves differences of embedded sets with a nonempty convex and mixed-type part in their visualisation.

Let us apply the Hermite interpolation piecewise on subintervals $I_i = [\widehat{\theta}_i, \widehat{\theta}_{i+1}]$ *where* $\widehat{\theta}_i = \frac{i}{N_k}$ *with* $i = 0, 1, \ldots, N_k = 2^k$*, multiplicities* $\mu_i = 2$*,* $i = 0, 1$*, and* $k = 0, 1, \ldots, 5$*. We shall test the theoretical result of Corollary 5.4. Herefore, test points* $\tau_j = \frac{j}{M}$*,* $j = 0, 1, \ldots, M$*, with* $M = 10 \cdot 2^5 = 320$ *are used to evaluate the error*

$$\varepsilon_k = \max_{j=0,\ldots,M} \|\overrightarrow{F}(\tau_j) - \overrightarrow{H_3}(\tau_j)\|$$

obtaining the results as in Table 1.

number of subintervals N_k	maximal error ε_k
1	6.982005e-03
2	5.280388e-04
4	3.666896e-05
8	2.421134e-06
16	1.556075e-07
32	9.863408e-09

Table 1: maximal error on test points for piecewise Hermite interpolation

The least square approximation of the logarithmic error bound $\log(C \cdot h^p)$ *in Table 1 with the unknown parameters* $\log(C)$ *and* p *yields the values* $C = 1.007620$ *and* $p = 3.893485$*. This last value is very close to the expected (theoretical) value* 4.0*.*

We highlight that in Example 7.2 the relation $F(t_1) \supseteq F(t_2)$ holds for any $t_1 \leq t_2$, therefore the visualised derivative $D\overrightarrow{F}(\cdot)$ contains the concave part, whereas in Examples 7.1 and 7.3 the other inclusion $F(t_1) \subseteq F(t_2)$ holds so that the convex part appears in the visualisation of the derivative.

Example 7.4 (cf. [Per07, Section 6.2.2]) *In the following example a rotating ellipsoid $\mathcal{E}$ is considered. We set $I = [0,1]$, $c = (0,0)$,*

$$Q = \begin{pmatrix} 4 & 0 \\ 0 & 1 \end{pmatrix} \quad \textit{and, finally,} \quad R(t) = \begin{pmatrix} \cos(\frac{\pi}{2} \cdot t) & -\sin(\frac{\pi}{2} \cdot t) \\ \sin(\frac{\pi}{2} \cdot t) & \cos(\frac{\pi}{2} \cdot t) \end{pmatrix}$$

The function then reads:

$$F(t) = R(t) \cdot \mathcal{E}(c,Q), \quad \mathcal{E}(c,Q) = \{x \in \mathbb{R}^n \,:\, \langle x, Q^{-1}x \rangle \leq 1\}$$

and its embedding is:

$$\overrightarrow{F}(t) = J_2(R(t) \cdot \mathcal{E}(c,Q))$$

The images of the set-valued map are strongly convex which results in a smooth case. Although the derivative has an empty convex and concave visualisation part, cf. Figure 5, its interpolant still has only convex images (which are no longer ellipsoids).

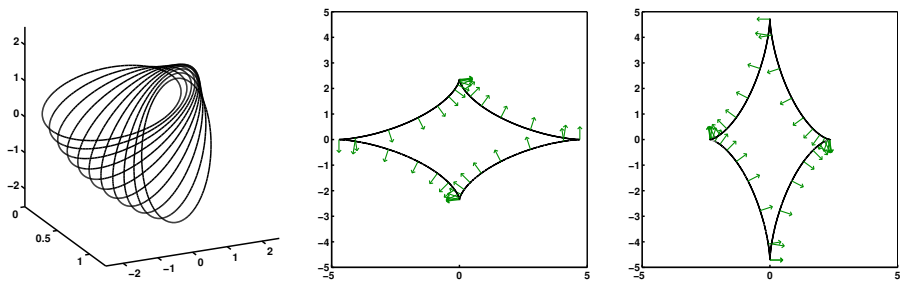

Figure 5: Funnel of $F(\cdot)$ and derivative data $D\overrightarrow{F}(0)$ and $D\overrightarrow{F}(1)$

The Hermite interpolation polynomial is computed around the point 0.5 *for shrinking intervals* $[0.5 - \frac{h_k}{2}, 0.5 + \frac{h_k}{2}]$, $h_k = 10^{-k}$, $k = 0,1,2,3$, *obtaining the results presented in Table 2. Clearly, the theoretical expected order of convergence* 4 *is achieved. The least square approximation of the logarithmic error*

interval for interpolation	maximal error ε_k
$[0.0, 1.0]$	5.740347e-01
$[0.45, 0.55]$	2.754315e-04
$[0.495, 0.505]$	2.838795e-08
$[0.4995, 0.5005]$	2.840173e-12

Table 2: maximal error for the Hermite interpolation at $\tau = 0.5$

bound $\log(C \cdot h^p)$ *in Table 2 with the unknown parameters* $\log(C)$ *and* p *yields the values* $C = 2.499332$ *and* $p = 3.790366$. *This value for* p *is close to the expected (theoretical) value 4.0. Only the first value for* ε_0 *in Table 2 is a rather good starting value for the error and disturbs slightly the gain of 4 digits after each step.*

In Figure 6, the values $F(\tau_i)$ of the original function and the values of the interpolant $\overrightarrow{H_3}(\tau_i)$ in $[0,1]$ are compared for $\tau_i = i \cdot 0.2$, $i = 1,2,3,4$ (shown in clockwise order for increasing index i); only for the values of $\overrightarrow{H_3}(\cdot)$, the corresponding normals are plotted. The interpolation achieves a good approximation of the original function.

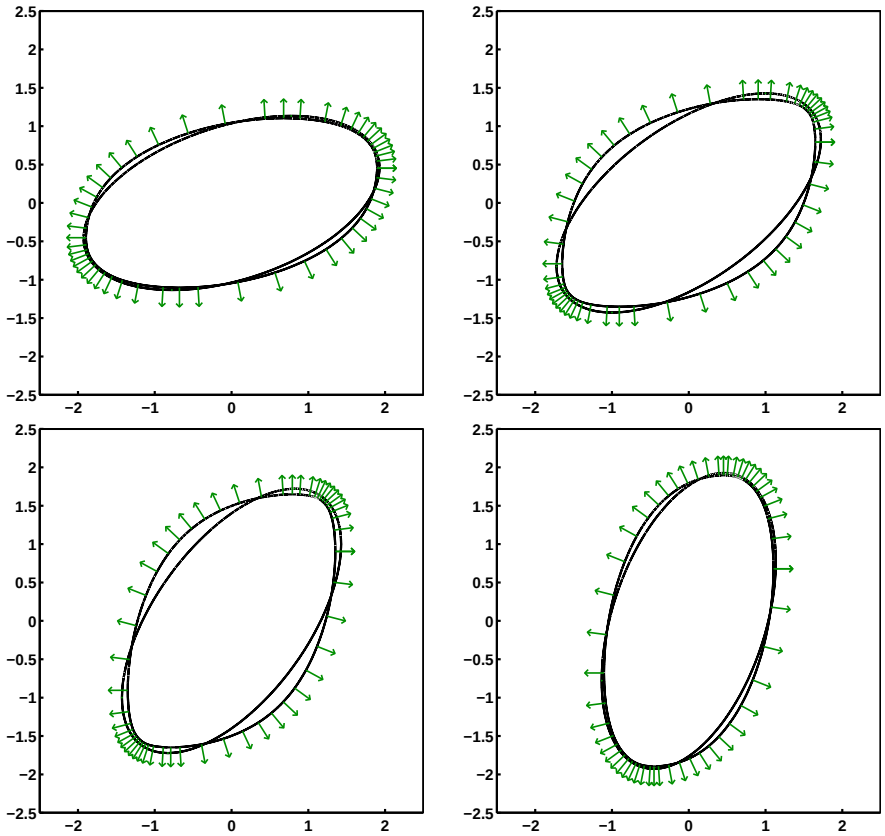

Figure 6: comparison of the intermediate values $F(\tau_i)$ and $\overrightarrow{H_3}(\tau_i)$, $i = 1, \ldots, 4$

Example 7.5 *An expanding ball moving along a curve $c(t) = (x(t), y(t))$ for $t \in I$ originates the convex-valued map:*

$$F : [0, \sqrt[4]{3}] \Longrightarrow \mathbb{R}^2 : t \mapsto B_{r(t)}(c(t)) \tag{50}$$

where $r(t) = \frac{1}{4}(\cos(2\pi(t+t_0)/t_0)+1)$, $x(t) = t^4 - 1$, $y(t) = t^5 - t$ and $t_0 = \sqrt[4]{3}$. We notice straight away that this is a smooth example by rewriting it as a sum of a scaled ball and a vector:

$$F(t) = r(t)B_1(0) + c(t) \tag{51}$$

which allows us to directly obtain the expression for its embedding and the its directed derivative

$$\overrightarrow{F}(t) = r(t) \cdot J_n(B_1(0)) + J_n(c(t)), \tag{52}$$

since the radius $r(t) \geq 0$. The derivative equals

$$D^\mu \overrightarrow{F}(t) = D^\mu r(t) \cdot J_n(B_1(0)) + J_n(D^\mu c(t)) \tag{53}$$

and is either an embedded ball or its inverse, depending on the sign of $D^\mu r(t)$. The derivative at the left and right endpoint of I is the embedded origin.

The error estimate on a test grid $\tau_i := 0.1 \cdot i \cdot t_0$ for $i = 0, 1, ..., 10$ delivers:

$$\max_{i=0,\ldots,10} \|\overrightarrow{F}(\tau_i) - \overrightarrow{H_3}(\tau_i)\| = 0.6447253 \tag{54}$$

This is a rather good accuracy, considering that the Hermite interpolating polynomial has only polynomial degree 3 and the enlargement of the sets as well as the 2D-movement of $\overrightarrow{F}(\cdot)$ in the phase space changes rapidly, cf. Figure 7.

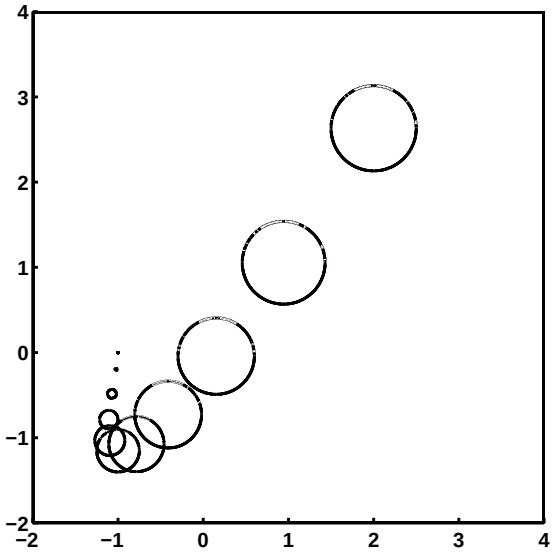

Figure 7: interpolated 2D-movement evaluated at the test points $(\tau_i)_{i=0,1,\ldots,10}$

In Figure 8, the linear, quadratic and Hermite interpolation of degree 3 (starting from the top to the bottom) are compared with the original function. In the left column, the 2D-movement in the phase space can be seen, whereas in the right column the t-y-projection of the interpolation polynomial is shown.

For this example, the error $\varepsilon = \max_{i=0,\ldots,10} \|\overrightarrow{F}(\tau_i) - \overrightarrow{P}(\tau_i)\|$ is calculated on the test grid for the various interpolation polynomials. The results are gathered in

type of interpolation	maximal error ε
linear	2.559469
quadratic	0.808878
Hermite	0.644725

Table 3: maximal error on test points for various interpolation polynomials

Table 3 and Figure 8. The best result is obtained by the Hermite interpolation.

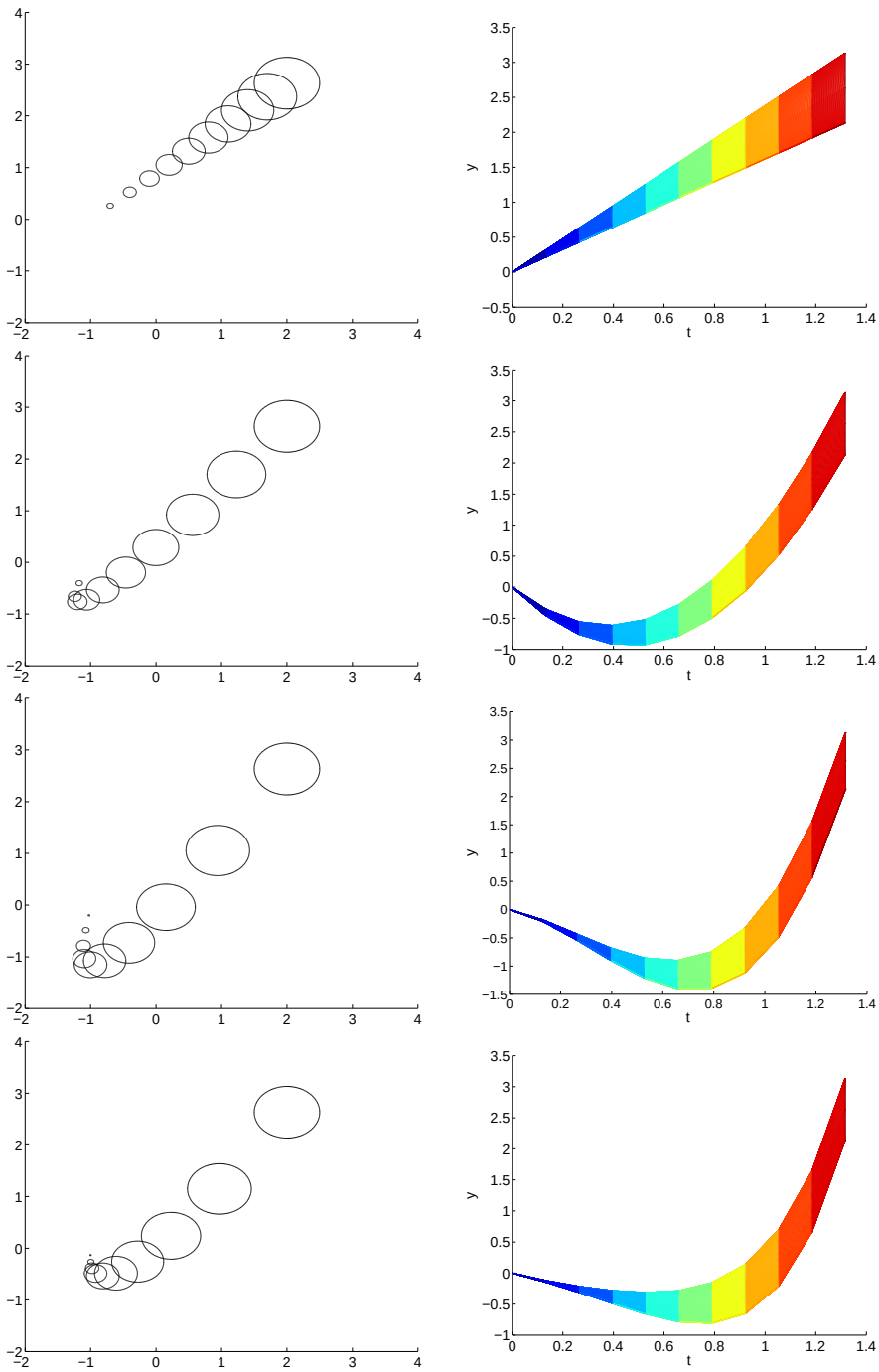

Figure 8: the linear, quadratic, Hermite interpolation and the original map

Conclusions

The Hermite interpolation of set-valued maps with the help of directed sets produces, as shown in the examples, good approximations to the original map. The derivatives and the interpolating polynomials which involve differences of embedded convex sets or their limits deliver very reasonable results. Although the derivative data at the left and right endpoints in the examples could be inverse to embedded convex sets or could even have nonconvex visualisation parts, the Hermite interpolation polynomial has as values always embedded convex images. These facts are by no means to be expected in the general case; the simple examples are chosen to produce those results and to demonstrate the possibilities of this approach with directed sets. For the simple case of constant and linear interpolation, it coincides with the usual set-valued interpolation; for higher polynomial degree it contains the interpolation based on support functions and on the geometric difference. In contrast to the latter approach, the images of the (directed) interpolation polynomial are always nonempty. In any case, the software that was used to perform the calculations also works if the interpolant has nonconvex visualisation parts.

Another advantage besides the visualisation is represented by the space of directed sets itself. It is a Banach space and is based on a recursive principle so that it is straight forward to carry over theoretical results from real-valued functions to the set-valued case, as for error estimates on the derivatives of the function and of its interpolant as well as for piecewise interpolation.

Acknowledgements: This work was partially supported by the Hausdorff Research Institute for Mathematics, Bonn within the HIM Junior Semester Program "Computational Mathematics" in February–April 2008.

References

[Art89] Z. Artstein. Piecewise Linear Approximation of Set-Valued Maps. *J. Approx. Theory*, 56(1):41–47, 1989.

[BB04] B. J. C. Baxter and R. Brummelhuis. Exponential Brownian motion and divided differences. Cambridge NA Report no. 06, Department of Applied Mathematics and Theoretical Physics, University of Cambridge, Cambridge, 2004.

[BF99] R. Baier and E. Farkhi. Directed Sets and Differences of Convex Compact Sets. In *Systems modelling and optimization, Proceedings of the* 18th *IFIP TC7 Conference held in Detroit, Michigan, July 22–25, 1997*, volume 396 of *Research Notes in Mathematics*, pages 135–143, Boca Raton–London–New York–Washington, D.C., 1999. Chapman and Hall/CRC.

[BF01a] R. Baier and E. Farkhi. Differences of Convex Compact Sets in the Space of Directed Sets, Part I: The Space of Directed Sets. *Set-Valued Anal.*, 9(3):217–245, 2001.

[BF01b] R. Baier and E. Farkhi. Differences of Convex Compact Sets in the Space of Directed Sets, Part II: Visualization of Directed Sets. *Set-Valued Anal.*, 9(3):247–272, 2001.

[BF01c] R. Baier and E. Farkhi. Directed Derivatives of Convex Compact-Valued Mappings. In N. Hadjisavvas and P. M. Pardalos, editors, *Advances in Convex Analysis and Global Optimization: Honoring the Memory of C. Caratheodory (1873–1950)*, volume 54 of *Nonconvex Optimization and Its Applications*, pages 501–514, Dordrecht-Boston-London, 2001. Kluwer Academic Publishers.

[BL94a] R. Baier and F. Lempio. Approximating Reachable Sets by Extrapolation Methods. In P. J. Laurent, A. Le Méhauteé, and L. L. Schumaker, editors, *Curves and Surfaces in Geometric Design*, pages 9–18. A K Peters, Wellesley, 1994.

[BL94b] R. Baier and F. Lempio. Computing Aumann's Integral. In A. B. Kurzhanski and V. M. Veliov, editors, *Modeling Techniques for Uncertain Systems, Proceedings of a Conferences held in Sopron, Hungary, July 6-10, 1992*, volume 18 of *Progress in Systems and Control Theory*, pages 71–92, Basel, 1994. Birkhäuser.

[Boc33] S. Bochner. Integration von Funktionen, deren Werte die Elemente eines Vektorraumes sind. *Fund. Math.*, XX:262–276, 1933.

[BSV68] G. Birkhoff, M. H. Schultz, and R. S. Varga. Piecewise Hermite interpolation in one and two variables with applications to partial differential equations. *Numer. Math.*, 11(3):232–256, 1968.

[CM96] C. Conti and R. Morandi. Piecewise C^1-shape-preserving Hermite interpolation. *Computing*, 56(4):323–341, 1996.

[CRE01] E. Cohen, R. F. Riesenfeld, and G. Elber. *Geometric Modeling with Splines: An Introduction.* A K Peters, Natick, Massachusetts, 2001.

[Dav75] P. J. Davis. *Interpolation and Approximation.* Dover Publications Inc., New York, 1975. Republication, with minor corrections, of the 1963 original.

[de 76] C. de Boor. Splines as Linear Combination of B-Splines. A Survey. In G.G. Lorentz, C.K. Chui, and L.L. Schumaker, editors, *Approximation Theory II*, pages 1–47, New York, 1976. Academic Press.

[de 01] C. de Boor. *A Practical Guide to Splines*, volume 27 of *Applied Mathematical Sciences.* Springer–Verlag, New York–Berlin–Heidelberg, 2001. Revised edition, original published in 1978.

[DF89] A. L. Dontchev and E. Farkhi. Error Estimates for Discretized Differential Inclusions. *Computing*, 41(4):349–358, 1989.

[DF90] T. D. Donchev and E. M. Farkhi. Moduli of Smoothness of Vector Valued Functions of a Real Variable and Applications. *Numer. Funct. Anal. Optim.*, 11(5 & 6):497–509, 1990.

[DH03] P. Deuflhard and A. Hohmann. *Numerical Analysis in Modern Scientific Computing. An introduction*, volume 43 of *Texts in Applied Mathematics.* Springer, New York–Berlin–Heidelberg, 2nd edition, 2003. First edition published in 1995.

[DKRV97] P. Diamond, P. Kloeden, A. Rubinov, and A. Vladimirov. Comparative Properties of Three Metrics in the Space of Compact Convex Sets. *Set-Valued Anal.*, 5(3):267–289, 1997.

[DL95] N. Dyn and D. Levin. Analysis of Hermite-type Subdivision Schemes. In C. K. Chui and L. L. Schumaker, editors, *Approximation theory VIII. Vol. 2. Wavelets and multilevel approximation. Proc. of the 8th Texas Internat. Conf. held at Texas A & M Univ., College Station, TX, January 8–12, 1995*, volume 6 of *Ser. Approx. Decompos.*, pages 117–124. World Scientific Publishing Co., Inc., River Edge, NJ, 1995.

[DR95] V. F. Demyanov and A. Rubinov. *Constructive Nonsmooth Analysis*, volume 7 of *Approximation & Optimization.* Peter Lang, Frankfurt am Main–Berlin–Bern–New York–Paris–Wien, 1995. Russian original "Foundations of nonsmooth analysis, and quasidifferential calculus" published in Nauka, Moscow, 1990.

[Fil04] L. Filipsson. Kergin Interpolation in Banach Spaces. *J. Approx. Theory*, 127(1):108–123, 2004.

[GA05] H. S. Goghary and S. Abbasbandy. Interpolation of fuzzy data by Hermite polynomial. *Int. J. Comput. Math.*, 82(5):595–600, 2005.

[GM82] M. Gasca and J. I. Maeztu. On Lagrange and Hermite interpolation in $\mathbf{R}^k$. *Numer. Math.*, 39(1):1–14, 1982.

[Gru05] R. E. Grundy. The application of Hermite interpolation to the analysis of non-linear diffusive initial-boundary value problems. *IMA J. Appl. Math.*, 70(6):814–838, 2005.

[GS00] M. Gasca and T. Sauer. On bivariate Hermite interpolation with minimal degree polynomials. *SIAM J. Numer. Anal.*, 37(3):772–798, 2000.

[Had50] H. Hadwiger. Minkowskische Addition und Subtraktion beliebiger Punktmengen und die Theoreme von Erhard Schmidt. *Math. Z.*, 53(3):210–218, 1950.

[HP74] E. Hille and R. S. Phillips. *Functional Analysis and Semi-Groups*, volume XXXI of *American Mathematical Society Colloquium Publications*. American Mathematical Society, Providence, Rhode Island, 1974. 3rd printing of revised edition of 1957, first edition published in 1947.

[HSS03] K. Hormann, S. Spinello, and P. Schröder. C^1-continuous Terrain Reconstruction from Sparse Contours. In T. Ertl, B. Girod, G. Greiner, H. Niemann, H.-P. Seidel, E. Steinbach, and R. Westermann, editors, *Proc. 8th Int. Worksh. Vision, Modeling, and Visualization*, pages 289–297. IOS Press, 2003.

[Kan74] K. Kansy. Elementare Fehlerdarstellung für Ableitungen bei der Hermite-Interpolation. *Numer. Math.*, 21(4):350–354, 1973/74.

[Kau80] E. Kaucher. Interval Analysis in the Extended Interval Space $\mathbb{IR}$. *Comput. Suppl.*, 2:33–49, 1980.

[Ker80] P. Kergin. A Natural Interpolation of C^k Functions. *J. Approx. Theory*, 29(4):278–293, 1980.

[Lem95] F. Lempio. Set-Valued Interpolation, Differential Inclusions, and Sensitivity in Optimization. In R. Lucchetti and J. Revalski, editors, *Recent Developments in Well-Posed Variational Problems*, volume 331 of *Mathematics and Its Applications*, pages 137–169, Dordrecht–Boston–London, 1995. Kluwer Academic Publishers.

[Low90] R. Lowen. A fuzzy Lagrange interpolation theorem. *Fuzzy Sets and Systems*, 34(1):33–38, 1990.

[LW04] Achan Lin and Marshall Walker. Proto-Bézier Simplices — Applications to Hermite Interpolation of Curves. In *Geometric Modeling and Computing: Seattle 2003*, Mod. Methods Math., pages 387–404. Nashboro Press, Brentwood, TN, 2004.

[MA96] S. Markov and Y. Akyildiz. Curve fitting and interpolation of biological data under uncertainties. *J.UCS*, 2(2):58–68 (electronic), 1996.

[Man01] C. Manni. On shape preserving C^2 Hermite interpolation. *BIT*, 41(1):127–148, 2001.

[Mar93] S. M. Markov. Some interpolation problems involving interval data. *Interval Comput./Interval. Vychisl.*, 3:164–182, 1993. Proceedings of the International Conference on Numerical Analysis with Automatic Result Verification (Lafayette, LA, 1993).

[Mar95] S. Markov. On the Directed Interval Arithmetic and Its Applications. *J.UCS*, 1(7):514–526, 1995.

[Mar00] S. Markov. On the Algebraic Properties of Convex Bodies and Some Applications. *J. Convex Anal.*, 7(1):129–166, 2000.

[MPSS96] S. M. Markov, E. Popova, U. Schneider, and J. Schulze. On linear interpolation under interval data. *Math. Comput. Simulation*, 42(1):35–45, 1996.

[Nik90a] M. S. Nikol′skiĭ. Approximation of a Continuous Multivalued Mapping by Constant Multivalued Mappings. *Moscow Univ. Comput. Math. Cybernet.*, 1:73–76, 1990.

[Nik90b] M. S. Nikol′skiĭ. Approximation of a Continuous Multivalued Mapping with Convex Range. *Sov. Math., Dokl.*, 40(2):406–409, 1990.

[Nik93] M. S. Nikol′skiĭ. Local approximation of first order to set-valued mappings. In A. B. Kurzhanski and V. M. Veliov, editors, *Set-valued Analysis and Differential Inclusions. A Collection of Papers resulting from a Workshop held in Pamporovo, Bulgaria, September, 1990*, volume 16 of *Progress in Systems and Control Theory*, pages 149–156. Birkhäuser Boston, Boston, MA, 1993.

[PBP02] H. Prautzsch, W. Böhm, and M. Palunszny. *Bézier and B-Spline Techniques*. Mathematics and Visualization. Springer, Berlin, 2002.

[Per03] G. Perria. Gerichtete Polytope: Arithmetische Operationen und Visualisierung mittels CGAL. Master's thesis, University of Bayreuth, Bayreuth, Germany, February 2003.

[Per07] G. Perria. *Set-Valued Interpolation*. Number 79 in Bayreuth. Math. Schr. Department of Mathematics, University of Bayreuth, Bayreuth, Germany, April 2007.

[Pet02] H. Petersson. Kergin interpolation in Banach spaces. *Studia Math.*, 153(2):101–114, 2002.

[Pon67] L. S. Pontryagin. Linear differential games. II. *Sov. Math., Dokl.*, 8(4):910–912, 1967.

[Pre71] P. M. Prenter. Lagrange and Hermite interpolation in Banach spaces. *J. Approx. Theory*, 4(4):419–432, 1971.

[PU02] D. Pallaschke and R. Urbański. *Pairs of compact convex sets. Fractional arithmetic with convex sets*, volume 548 of *Mathematics and Its Applications*. Kluwer Academic Publishers, Dordrecht, 2002.

[RA92] A. M. Rubinov and I. S. Akhundov. Difference of compact sets in the sense of Demyanov and its application to non-smooth analysis. *Optimization*, 23(3):179–188, 1992.

[Roc72] R. T. Rockafeller. *Convex Analysis*, volume 28 of *Princeton Mathematical Series*. Princeton University Press, Princeton, NJ, 1972. 2nd edition, first edition in 1970.

[Sau95] Thomas Sauer. Multivariate B-Splines with (almost) Arbitrary Knots. In C. K. Chui and L. L. Schumaker, editors, *Approximation Theory VIII, Vol. 1. Approximation and Interpolation. Proc. of the 8th Texas Internat. Conf. held at Texas A & M Univ., College Station, TX, January 8–12, 1995*, volume 6 of *Ser. Approx. Decompos.*, pages 477–488. World Scientific Publishing Co., Inc., 1995.

[Sch93] R. Schneider. *Convex Bodies: The Brunn-Minkowski Theory*, volume 44 of *Encyclopedia of Mathematics and Its Applications*. Cambridge University Press, Cambridge, 1993.

[Sim08] S. Simon. Kergin approximation in Banach spaces. *J. Approx. Theory*, 154(2):181–186, 2008.

[SX95] T. Sauer and Yuan Xu. On Multivariate Hermite Interpolation. *Adv. Comput. Math.*, 4(3):207–259, 1995.

[Vel89a] V. M. Veliov. Discrete Approximations of Integrals of Multivalued Mappings. *C. R. Acad. Bulgare Sci.*, 42(12):51–54, 1989.

[Vel89b] V. M. Veliov. Second order discrete approximations to strongly convex differential inclusions. *Systems Control Lett.*, 13(3):263–269, 1989.

[Vel92] V. M. Veliov. Second Order Discrete Approximation to Linear Differential Inclusions. *SIAM J. Numer. Anal.*, 29(2):439–451, 1992.

[Vit79] R. A. Vitale. Approximation of Convex Set-Valued Functions. *J. Approx. Theory*, 26(4):301–316, 1979.

[Wal97] S. Waldron. Integral Error Formulæ for the Scale of Mean Value Interpolations which Includes Kergin and Hakopian Interpolation. *Numer. Math.*, 77(1):105–122, 1997.